Chapter 4 Results and Discussion

4.1 Chapter Overview

Thirty-one data series studied to find out the OGE during single discharge, dual discharge, triple discharge, quadruple discharge and quintuple discharge conditions. The result of data series are presented for various branch combinations. Single discharge and dual discharge data series are compared to the correlations and experimental results that of available in previous investigations. Empirical correlations were developed, but their accuracy ascertained for the range of conditions covered in this investigation. These correlations have the coefficient of determination, R-squared, value 96 percentage or more. The high value of R-squared suggests the experimental data are closely fitted to the regression line.

4.2 Test Matrix of the Experiment

Table 4.1 gives the test matrix for the single, dual, triple, quadruple, and quintuple discharges. Series nos. 1-1 to 1-5 explored the effect of Fr_L during single discharge condition for the five branches of the test piece. In case of dual discharge, triple discharge and quadruple discharge conditions, series nos. 2-1 to 2-10, series nos. 3-1 to 3-10 and series nos. 4-1 to 4-5 explored the effect of Fr_L for various branch combinations respectively. Series no. 5-1 explored the effect of Fr_L for quintuple discharge condition. Within the range of Fr_L total eight observations were

Table 4.1: Test matrix for experimental investigation

Sr. no.	Series no.	Activated branch/es	Set no.	Fr_L	Total number of OGEs
1	1-1	B1 only	1-1.1 to 1-1.8	6.4 to 27.5	8
2	1-2	B2 only	1-2.1 to 1-2.8		8
3	1-3	B3 only	1-3.1 to 1-3.8		8
4	1-4	B4 only	1-4.1 to 1-4.8		8
5	1-5	B5 only	1-5.1 to 1-5.8		8
6	2-1	B1 and B2	2-1.1 to 2-1.8	6.4 to 27.5	16
7	2-2	B1 and B3	2-2.1 to 2-2.8		16
8	2-3	B1 and B4	2-3.1 to 2-3.8		16
9	2-4	B1 and B5	2-4.1 to 2-4.8		16
10	2-5	B2 and B3	2-5.1 to 2-5.8		16
11	2-6	B2 and B4	2-6.1 to 2-6.8		16
12	2-7	B2 and B5	2-7.1 to 2-6.8		16
13	2-8	B3 and B4	2-8.1 to 2-8.8		16
14	2-9	B3 and B5	2-9.1 to 2-9.8		16
15	2-10	B4 and B5	2-10.1 to 2-10.8		16
16	3-1	B1, B2 and B3	3-1.1 to 3-1.8	6.4 to 27.5	24
17	3-2	B1, B2 and B4	3-2.1 to 3-2.8		24
18	3-3	B1, B2 and B5	3-3.1 to 3-3.8		24
19	3-4	B1, B3 and B4	3-4.1 to 3-4.8		24
20	3-5	B1, B3 and B5	3-5.1 to 3-5.8		24
21	3-6	B1, B4 and B5	3-6.1 to 3-6.8		24
22	3-7	B2, B3 and B4	3-7.1 to 3-7.8		24
23	3-8	B2, B3 and B5	3-8.1 to 3-8.8		24
24	3-9	B2, B4 and B5	3-9.1 to 3-9.8		24
25	3-10	B3, B4 and B5	3-10.1 to 3-10.8		24
26	4-1	B1, B2, B3 and B4	4-1.1 to 4-1.8	6.4 to 27.5	32
27	4-2	B1, B2, B3 and B5	4-2.1 to 4-2.8		32
28	4-3	B1, B2, B4 and B5	4-3.1 to 4-3.8		32
29	4-4	B1, B3, B4 and B5	4-4.1 to 4-4.8		32
30	4-5	B2, B3, B4 and B5	4-5.1 to 4-5.8		32
31	5-1	B1, B2, B3, B4 and B5	5-1.1 to 5-1.8	6.4 to 27.5	40

taken for each branch for various discharge conditions. Appendix B gives the complete tabulation of all the experimental data.

4.3 Gas Entrainment Phenomena

The section discusses the gas entrainment phenomena for the simple case of single discharges and complex case of quintuple discharge experiments through visual observations. For dual discharge, triple discharge, and quadruple discharge conditions, images of typical gas entrainment phenomena is given in Appendix D.

4.3.1 Typical Gas entrainment phenomena for single discharge experiment

The experiments revealed that OGE depends on Fr_L of the branch and the interface height in the header. The gas entrainment phenomenon is described by Froude number of liquid phase at side branch and form of interface. During the study of gas entrainment at side branch B1 of set no. 1-1.1, the interface height 'h' was flat when liquid height was well above the branch as shown in Figure 4.1(a). As the interface was lowered, initial depression was formed in the flat surface of interface as shown in Figure 4.1(b). The Froude number of the branch was $Fr_{L,B1}$. Further, with slight decrease in the interface height, hair-thin gas tube emerged suddenly at the bottom of the depression and jumped into B1 as shown in Figure 4.1(c). The gas started flowing into B1. The visual observation showed that at that position the flow was vortex. Soon after, the vortex disappeared and stopped the gas flow into B1. This gas entrainment mode is termed as unsteady entrainment, as initially the gas started flowing into the branch and then failed to flow continuously as shown in Figure 4.1(d). Further lowering the interface level, a critical height of the interface was

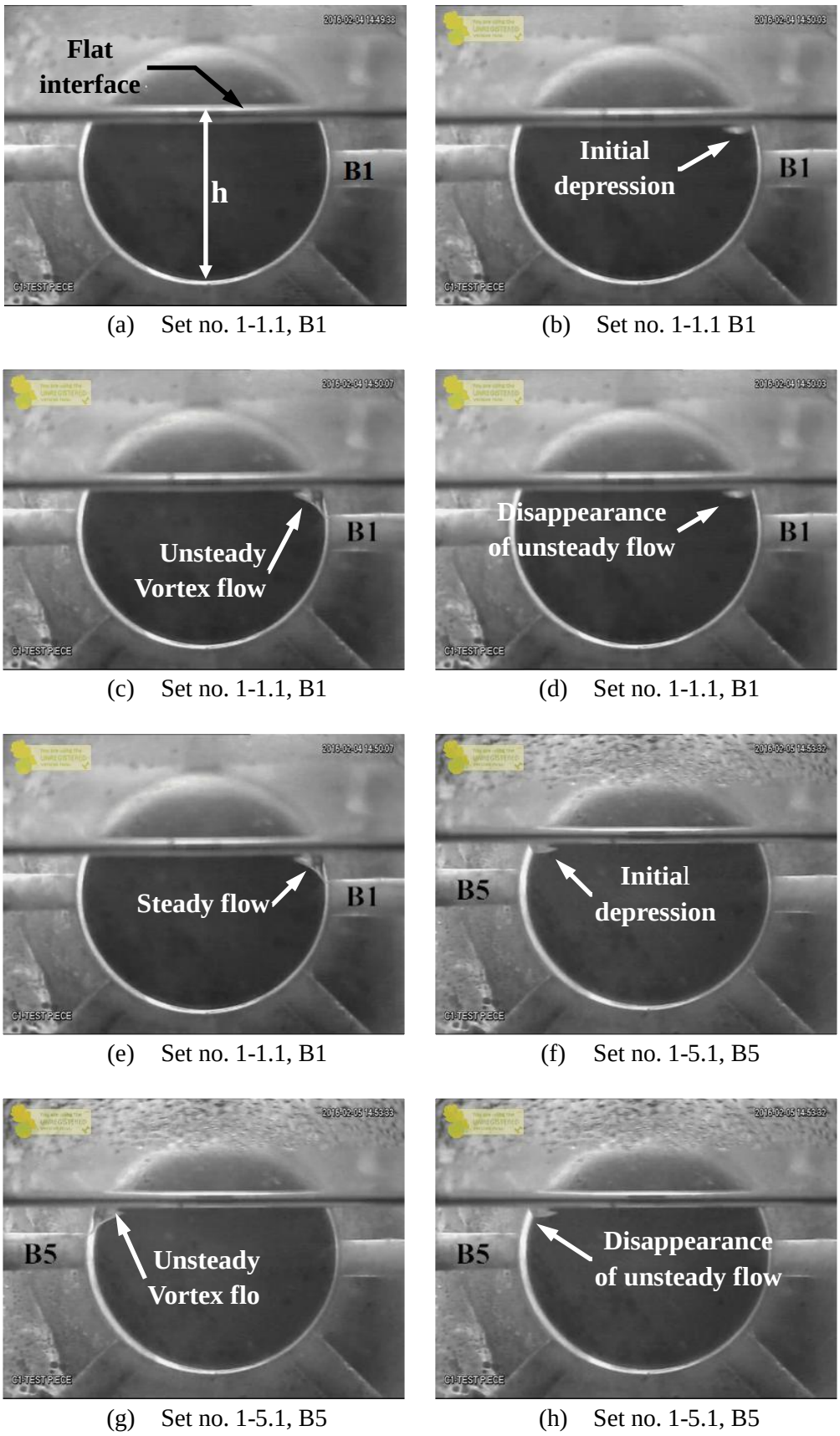

(a) Set no. 1-1.1, B1 (b) Set no. 1-1.1 B1

(c) Set no. 1-1.1, B1 (d) Set no. 1-1.1, B1

(e) Set no. 1-1.1, B1 (f) Set no. 1-5.1, B5

(g) Set no. 1-5.1, B5 (h) Set no. 1-5.1, B5

Figure 4.1: Gas entrainment phenomena of single discharge experiment

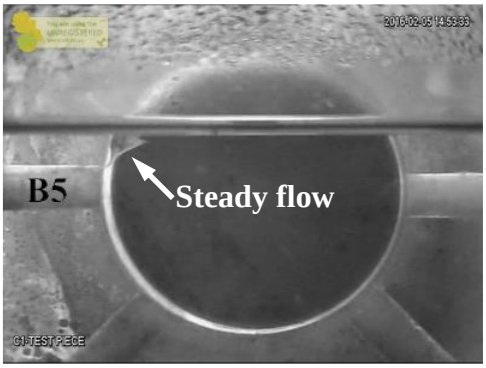

(i) Set no. 1-5.1, B5

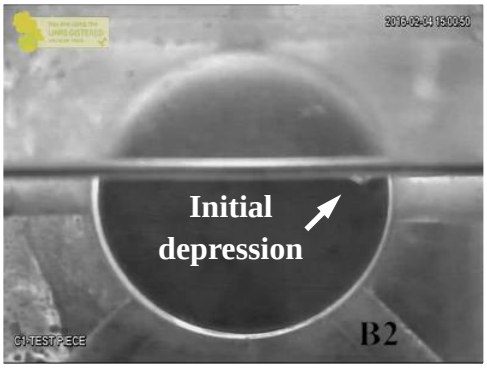

(j) Set no. 1-2.1, B2

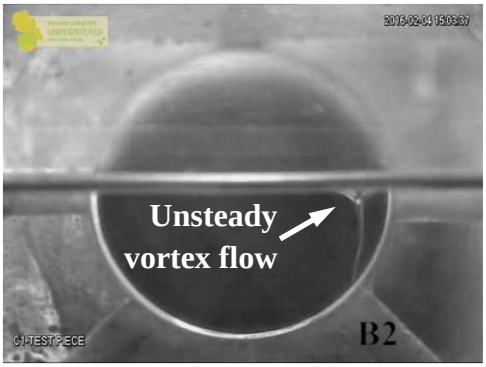

(k) Set no. 1-2.1, B2

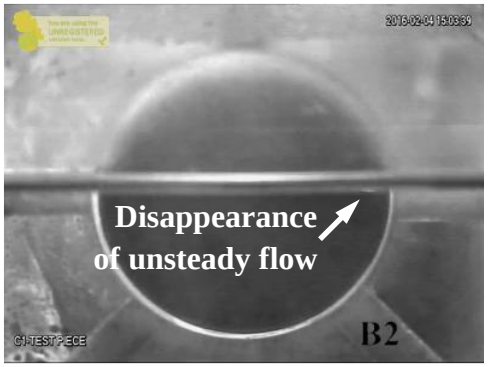

(l) Set no. 1-2.1, B2

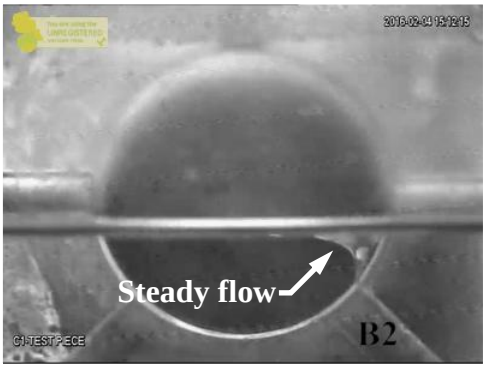

(m) Set no. 1-2.1, B2

(n) Set no. 1-4.1, B4

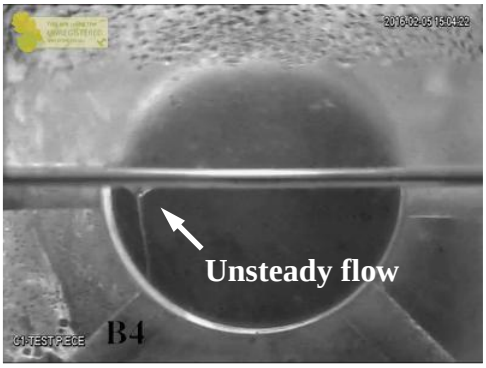

(o) Set no. 1-4.1, B4

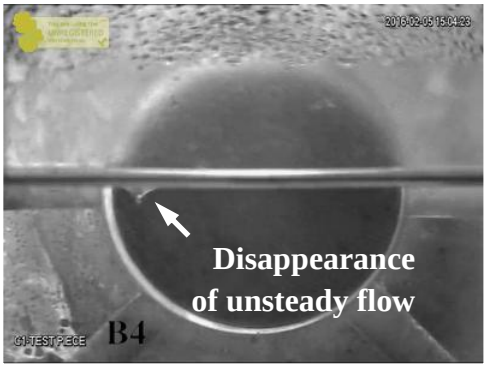

(p) Set no. 1-4.1, B4

Figure 4.1: Gas entrainment phenomena of single discharge experiment (cont.)

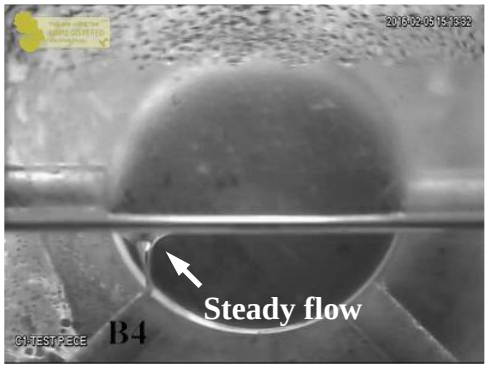

(q) Set no. 1-4.1, B4

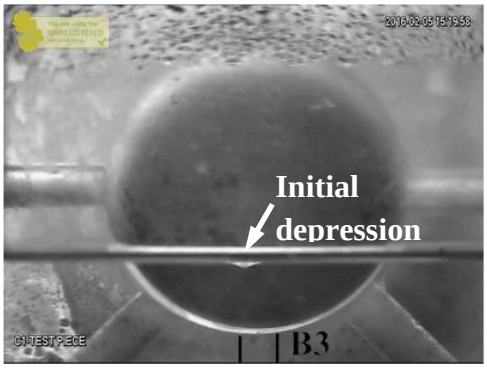

(r) Set no. 1-3.1, B3

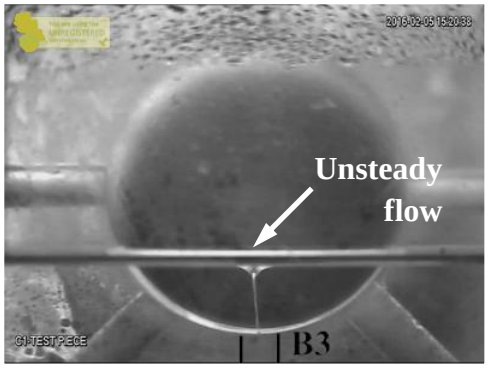

(s) Set no. 1-3.1, B3

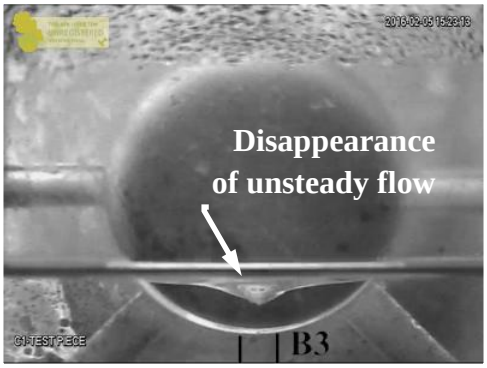

(t) Set no. 1-3.1, B3

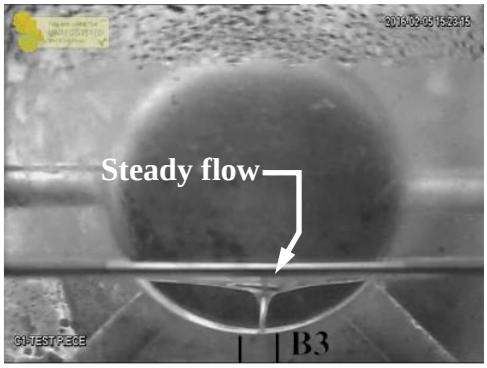

(u) Set no. 1-3.1, B3

Figure 4.1: Gas entrainment phenomena of single discharge experiment (cont.)

reached and yet again suddenly, a hair-thin gas tubes emerged from the bottom of the depressions reaching to B1. At this instance, the flow of gas into B1 was continuous and did not disappear with further lowering of the interface height. This mode of gas entrainment is termed as steady gas entrainment as shown in Figure 4.1(e). The visual observation showed that at that instance, the gas entrainment was vortex-free. The unsteady gas entrainment occurred several times before steady gas entrainment occurs, therefore, a steady gas entrainment condition identified as the OGE. The thin gas tube carried little quantity of the gas from the header, thus the pressure in the phase separator did not rise. The Froude number for B1 was $Fr_{L,B1} = Fr_{LOGE,B1}$. Set no. 1-5.1 of B5 showed identical gas entrainment phenomena to set no. 1-1.1 as shown in Figure 4.1(f) to Figure 4.1(i). The Froude number of the branch was $Fr_{L,B5} = Fr_{LOGE,B5}$. Set nos. 1-1.2 to 1-1.8 and 1-5.2 to 1-5.8 demonstrated similar gas entrainment phenomena to the set nos. 1-1.1 for different Fr_L.

Set nos. 1-2.1, 1-3.1, and 1-4.1 of B2, B3, and B4 respectively, demonstrated similar stages of gas entrainment phenomena to set no. 1-1.1 of B1 as shown in Figure 4.1(j) to Figure 4.1(u). The Froude number of the branches were $Fr_{L,B2} = Fr_{LOGE,B2}$, $Fr_{L,B3} = Fr_{LOGE,B3}$, and $Fr_{L,B4} = Fr_{LOGE,B4}$. The stages of gas entrainment phenomena for set nos. 1-2.2 to 1-2.8, 1-3.2 to 1-3.8, and 1-4.2 to 1-4.8 were observed similar to set nos. 1-2.1, 1-3.1, and 1-4.1 respectively.

4.3.2 Typical Gas entrainment phenomena for quintuple discharge experiment

The general phenomenon of the gas entrainment for the quintuple discharge condition is discussed in the present section. The images of interface shapes are represented for the set no. 5-1.1 as shown in Figure 4.2.

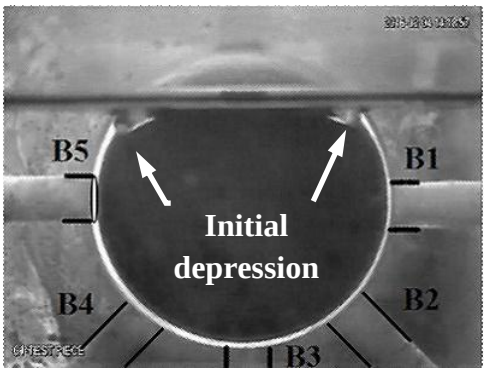

(a) Set no. 5-1.1, B1 and B5

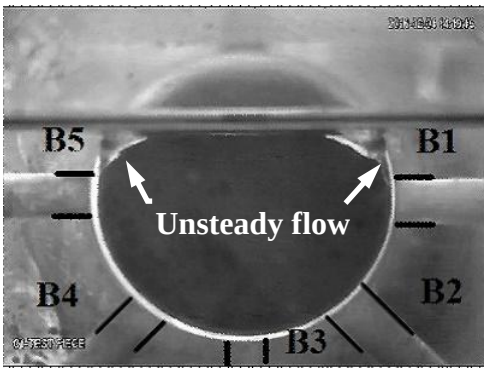

(b) Set no. 5-1.1, B1 and B5

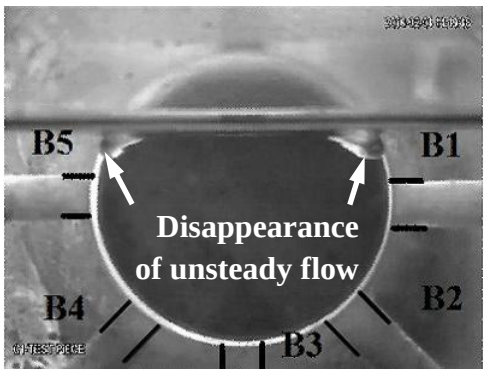

(c) Set no. 5-1.1, B1 and B5

a

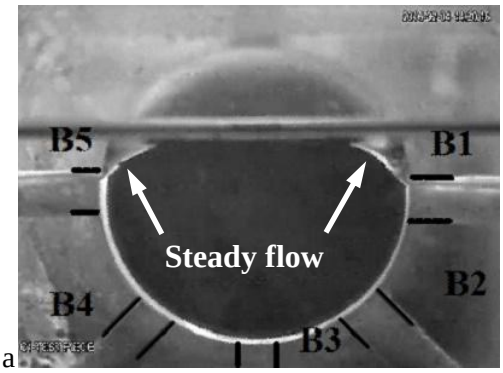

(d) Set no. 5-1.1, B1 and B5

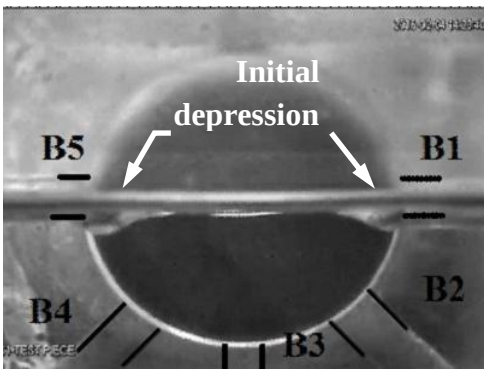

(e) Set no. 5-1.1, B2 and B4

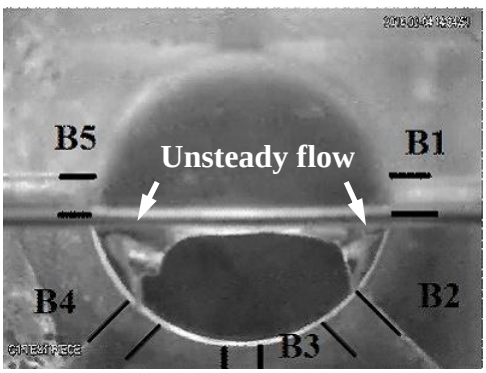

(f) Set no. 5-1.1, B2 and B4

Figure 4.2: Gas entrainment phenomena of quintuple discharge experiment

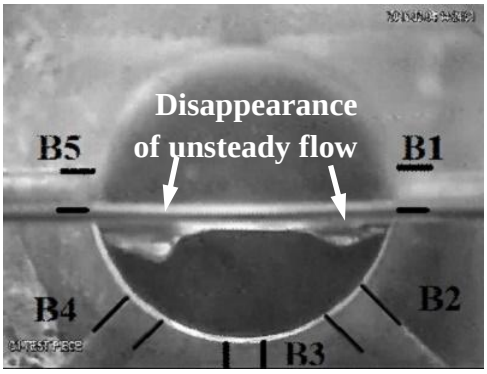

(g) Set no. 5-1.1, B2 and B4

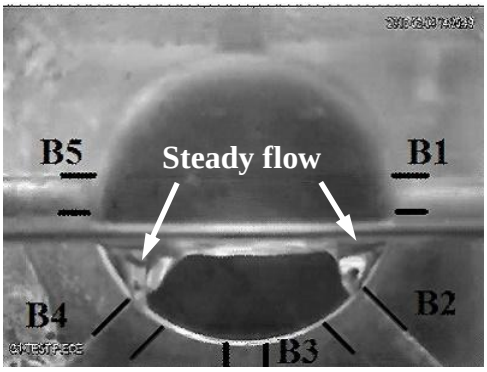

(h) Set no. 5-1.1, B2 and B4

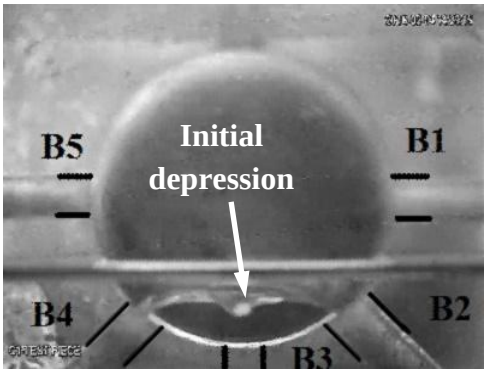

(i) Set no. 5-1.1, B3

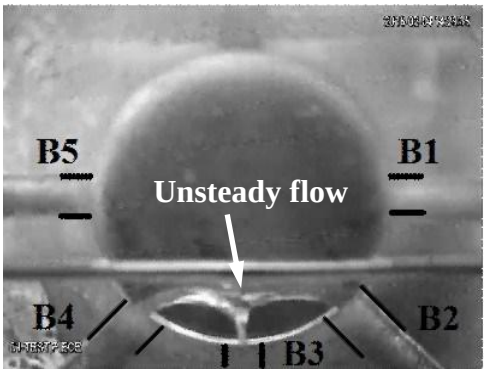

(j) Set no. 5-1.1, B3

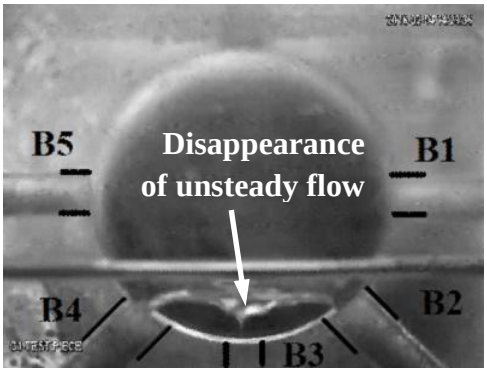

(k) Set no. 5-1.1, B3

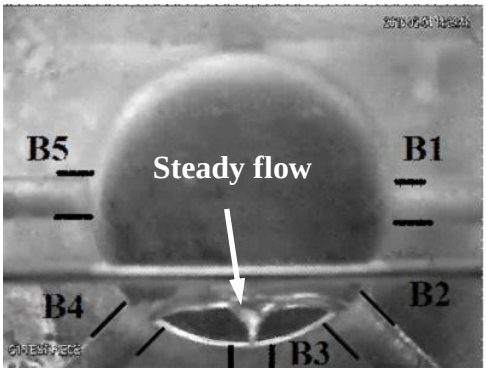

(l) Set no. 5-1.1, B3

Figure 4.2: Gas entrainment phenomena of quintuple discharge experiment (cont.)

The set nos. 5-1.2 to 5-1.8 of quintuple discharge has similar gas entrainment phenomena to set no. 5-1.1 for different Fr_L. The interface was flat when the liquid height was well above the side branches B1 and B5 as shown in Figure 4.2(a). The Froude numbers were same, i.e. $Fr_{L,B1} = Fr_{L,B2} = Fr_{L,B3} = Fr_{L,B4} = Fr_{L,B5}$. As the interface was lowered, initial depressions in the flat interface surface were viewed, and gradually deepened with the fall in interface height as shown in Figure 4.2(b). Further, with a slight decrease in the interface height, a hair-thin gas tube emerged suddenly at the bottom of the deepened depressions and jumped into B1 and B5 as shown in Figure 4.2(c). The gas started flowing into B1 and B5 from the thin gas tube. The visual observation showed that at that position the flow was a vortex. Soon after, the vortex disappeared and stopped the gas flow into B1 and B5. This gas entrainment mode is termed as unsteady entrainment, as initially the gas started flowing into the branch and then failed to flow continuously as shown in Figure 4.2(d).

Further lowering the interface level, a critical height of the interface was reached and yet again suddenly, two hair-thin gas tubes emerged from the bottom of the depressions reaching to B1 and B5. At this instance, the flow of gas into B1and B5 was continuous and did not disappear with further lowering of the interface height. This mode of gas entrainment is termed as steady entrainment as shown in Figure 4.2(e). Visual observation showed at that position, the gas entrainment was vortex-free. The unsteady gas entrainment occurred several times before steady gas entrainment occurs; therefore, a steady gas entrainment condition is identified as the OGE. The thin gas tube carried a little quantity of the gas from the header, thus the pressure in the phase separator did not rise. The Froude number of the branches were $Fr_{L,B1} = Fr_{L,B2} = Fr_{L,B3} = Fr_{L,B4} = Fr_{L,B5} = Fr_{LOGE,B1} = Fr_{LOGE,B5}$.

Further decrease in the interface height, it was found that gas flow rate from B1 and B5 have increased. The stages of gas entrainment phenomena for B2 and B4 were observed similar to that of B1 and B5 as shown in Figure 4.2(f) to Figure 4.2(i). The Froude number of the branches were $Fr_{L,B2} = Fr_{L,B3} = Fr_{L,B4} = Fr_{LOGE,B2} = Fr_{LOGE,B4}$. B3 showed the similar stages of gas entrainment phenomena as that shown in Figure 4.2(j) to Figure 4.2(m) and the Froude number was $Fr_{L,B3} = Fr_{LOGE,B3}$.

In the case Froude number higher than 6.4, the stages of gas entrainment phenomena were similar to that of Fr_L = 6.4, except that it occurred at a relatively higher height. OGE was determined by slowly decreasing the interface level at the rate of 1 mm in 5 seconds to keep steady experimental condition.

4.4 Single Discharge Experiments

Single discharge experiments were carried out with opening one branch at a time and by varying Fr_L to find out the OGE. The results thus obtained are then plotted and compared with that of the previous investigations. New empirical correlations are then developed for side, inclined, and bottom branches.

4.4.1 Presentation of data and correlations

The cases of geometrically identical and unique branch combinations are presented in Table 4.2

Table 4.2: Cases of geometrically identical and unique branch combinations of single discharge

Case no.	Series no.	Branch combinations		
		Side Branch	Inclined Branch	Bottom Branch
1-A	1-1	B1	X	X
	1-5	B5	X	X
1-B	1-2	X	B2	X
	1-4	X	B4	X
1-C	1-3	X	X	B3

Figure 4.3 shows the results for the dimensionless critical gas entrainment height for the single discharge experiment. The following are empirical correlations developed for critical height of each branch during a single discharge condition.

Case no. 1-A: Activated side branches, i.e. B1 of series no. 1-1 and B5 of series no. 1-5.

$$\frac{h_{OGE}}{d} = 0.557\ Fr_L^{0.4} \tag{4.1}$$

Case no. 1-B: Activated inclined branches, i.e. B2 of series no. 1-2 and B4 of series no. 1-4.

$$\frac{h_{OGE}}{d} = 0.641\ Fr_L^{0.4} \tag{4.2}$$

Case no. 1-C: Activated bottom branch, i.e. B3 of series no. 1-3.

$$\frac{h_{OGE}}{d} = 0.582\ Fr_L^{0.4} \tag{4.3}$$

For the case no. 1-A, case no. 1-B, and case no. 1-C the Root Mean Square Deviation (RMSD) is given in Table 4.3, when comparing the correlation and experimental values of $\frac{h_{OGE}}{d}$ over the range of branch Froude number. The RMSD in percentage was calculated as,

$$\text{RMSD}\ (\%) = \pm\sqrt{\left(\frac{1}{N}\sum_{i=1}^{i=N}\left|\frac{h_{OGE(Experiement)_i} - h_{OGE(Correlation)_i}}{h_{OGE(Experiement)_i}}\right|^2\right)}\ \text{X}\ 100 \tag{4.4}$$

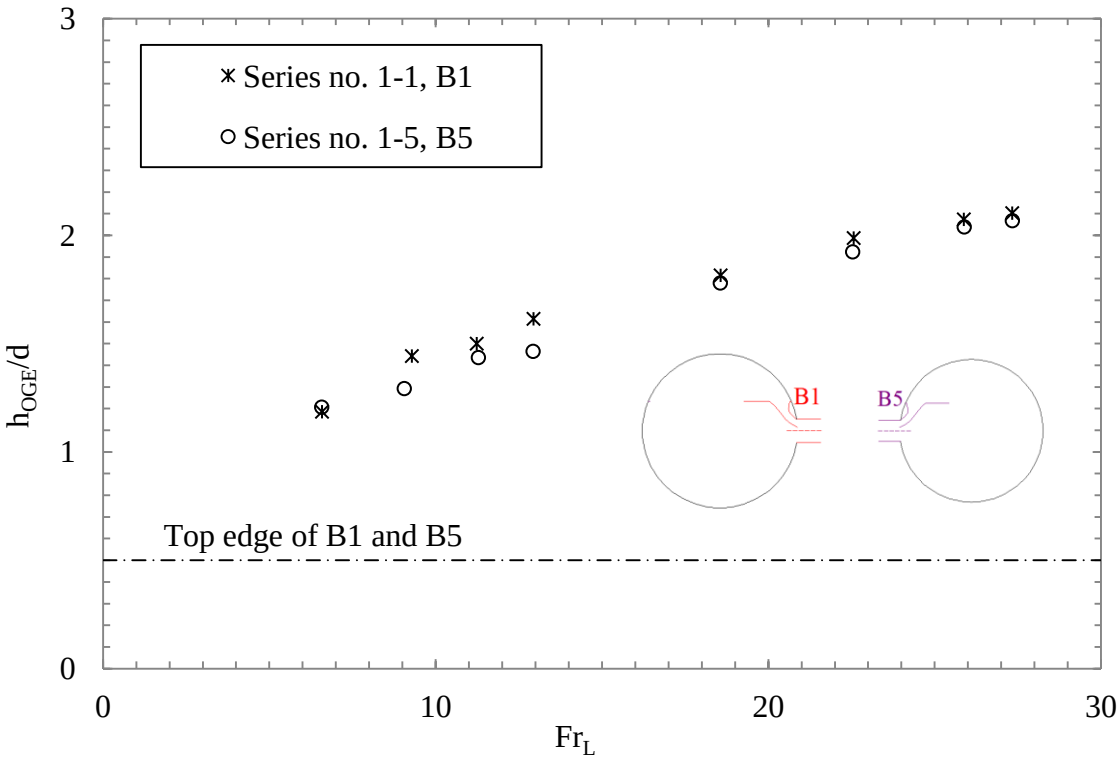

(a) Case no. 1-A

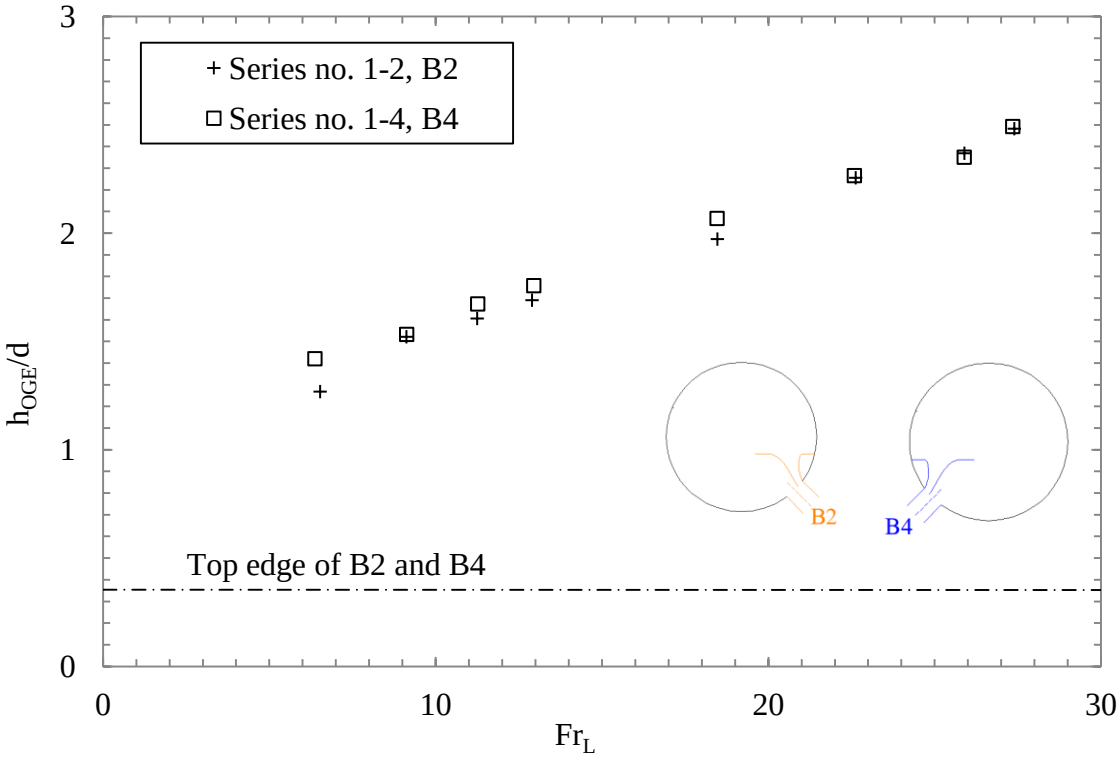

(b) Case no. 1-B

Figure 4.3: Interface level at the OGE of single discharge experiment

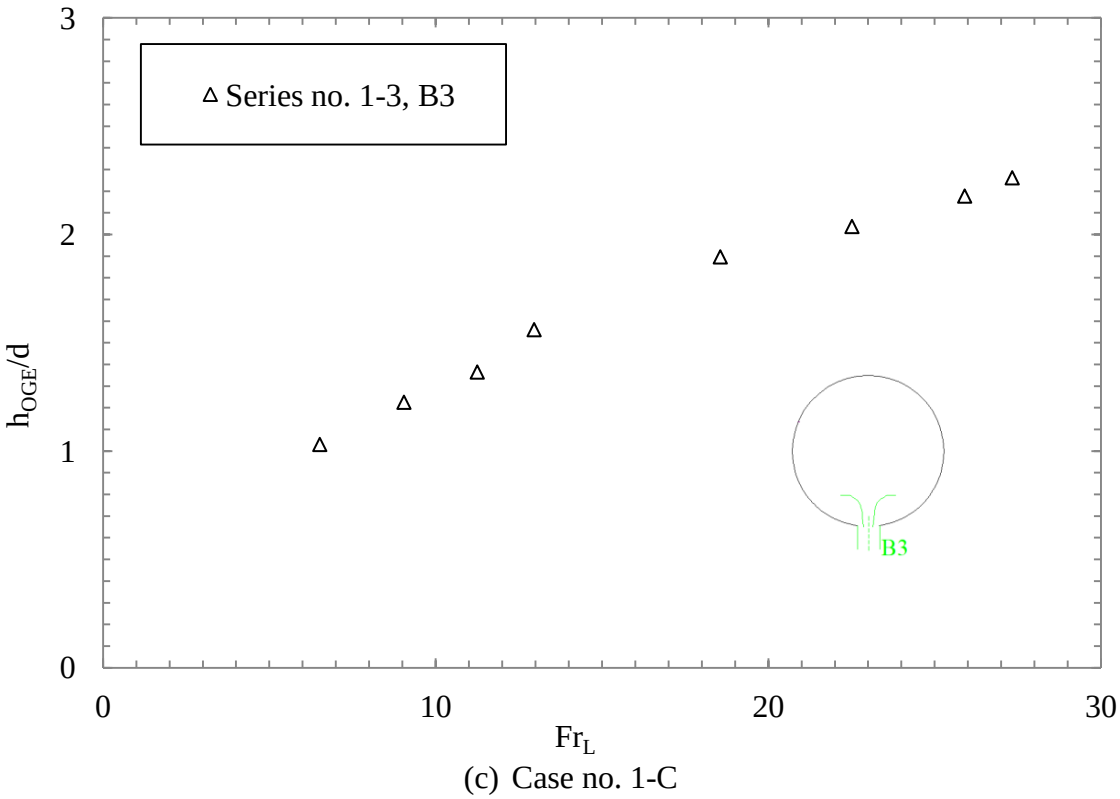

(c) Case no. 1-C

Figure 4.3: Interface level at the OGE of single discharge experiment (cont.)

Table 4.3: Correlation constants and RMSD for single discharge

Case no.	Series no.	Activated branch	Correlation constants		RMSD (%)
			C_1	C_2	
1-A	1-1 and 1-5	Side	0.557	0.4	±7.2
1-B	1-2 and 1-4	Inclined	0.641	0.4	±7.9
1-C	1-3 only	Bottom	0.582	0.4	±6.0

The general observation from Figure 4.3 is that the critical height of the branches changed markedly with the position of the branch. However, it was observed that there is similarity in critical height for the geometrically identical branches as shown in Figure 4.3(a) and Figure 4.3(b). Comparison of coefficients of correlations for case nos. 1-A, 1-B, and 1-C (Equations 4.1, 4.2 and 4.3) show that value of $\frac{h_{OGE}}{d}$ increases from side branches to bottom branch to inclined branches. Thus, strongest OGE was seen in inclined branches compared to bottom branch and side branches. This trend has some bearing on the multiple discharge experiments.

4.4.2 Comparison of present data with existing correlations

Figure 4.4 compares the present results and already existing correlations for side, inclined, and bottom branches. Correlations used in these figures are given in Chapter 2. Table 4.4 depicts a comparison of present data with existing correlations. Significant deviation is seen among the existing correlations. Experimental data of side branches were in good agreement with the Hassan et al. (1998) and Bartley et al. (2011) with the deviation of ±3.4 percentage and ±4.1 percentage respectively as shown in Figure 4.4(a). Present data for inclined branches were compared with that of Bowden and Hassan (2011) and is given in Figure 4.4(b), it should be noted that this is the only correlation available in the open literature for the purpose of comparison. For bottom branch, the present experimental results were found closer to that of Bowden and Hassan (2011) and Lubin and Hurwitz (1966) as shown in Figure 4.4(c).

As depicted in Table 2.1, the correlation constant C_1 of Yonomoto and Tasaka (1988) showed the trend of increase of C_1 as we move from the side branch to the bottom branch. Equations (4.1) and (4.3) showed the similar trend of increase of C_1.

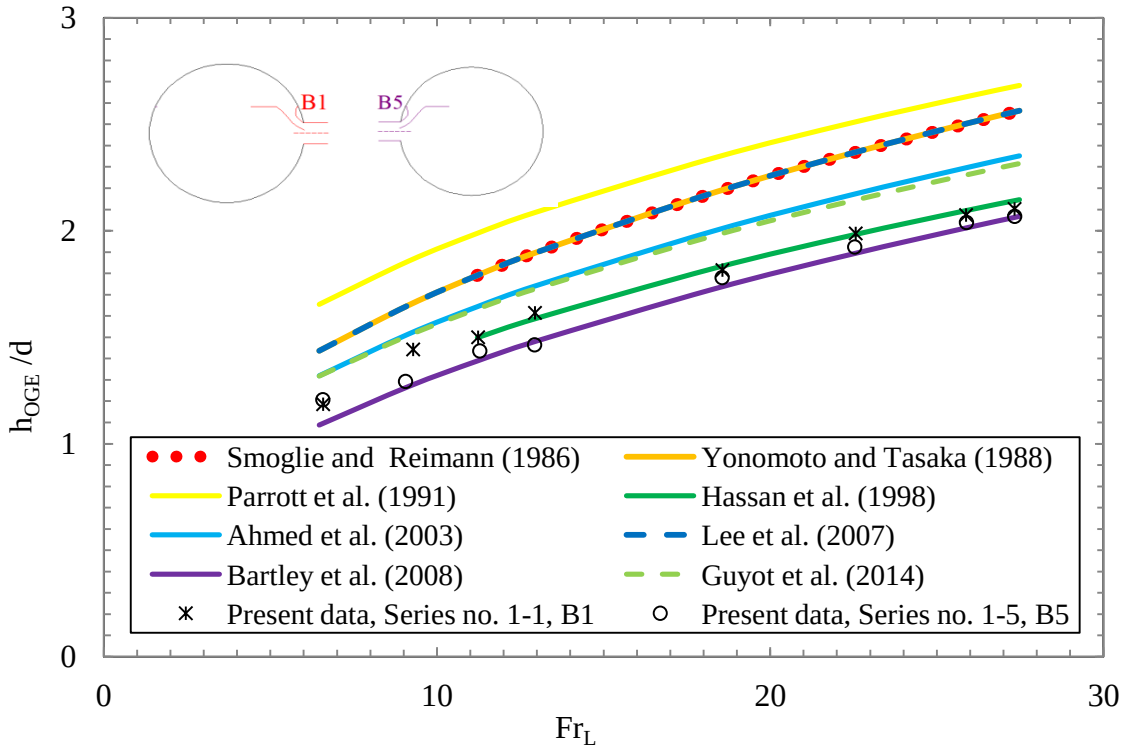

(a) For side branches

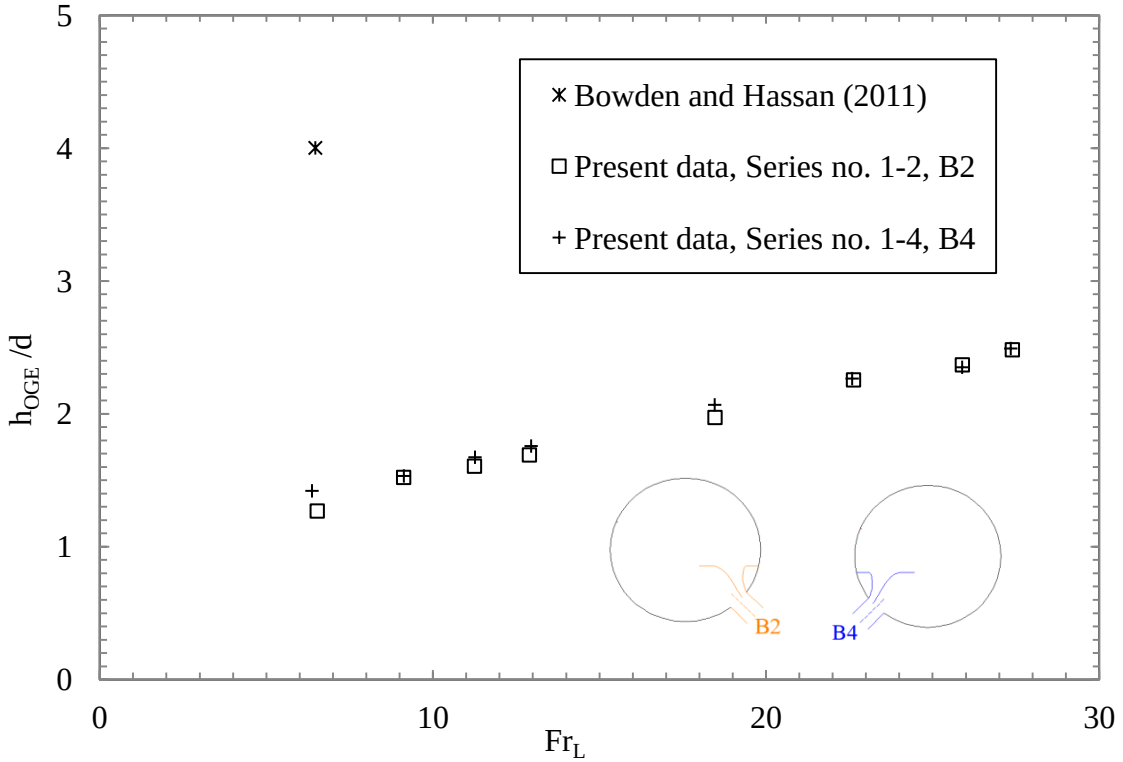

(b) For inclined branches

Figure 4.4: Comparison of present data with existing correlations of single discharge

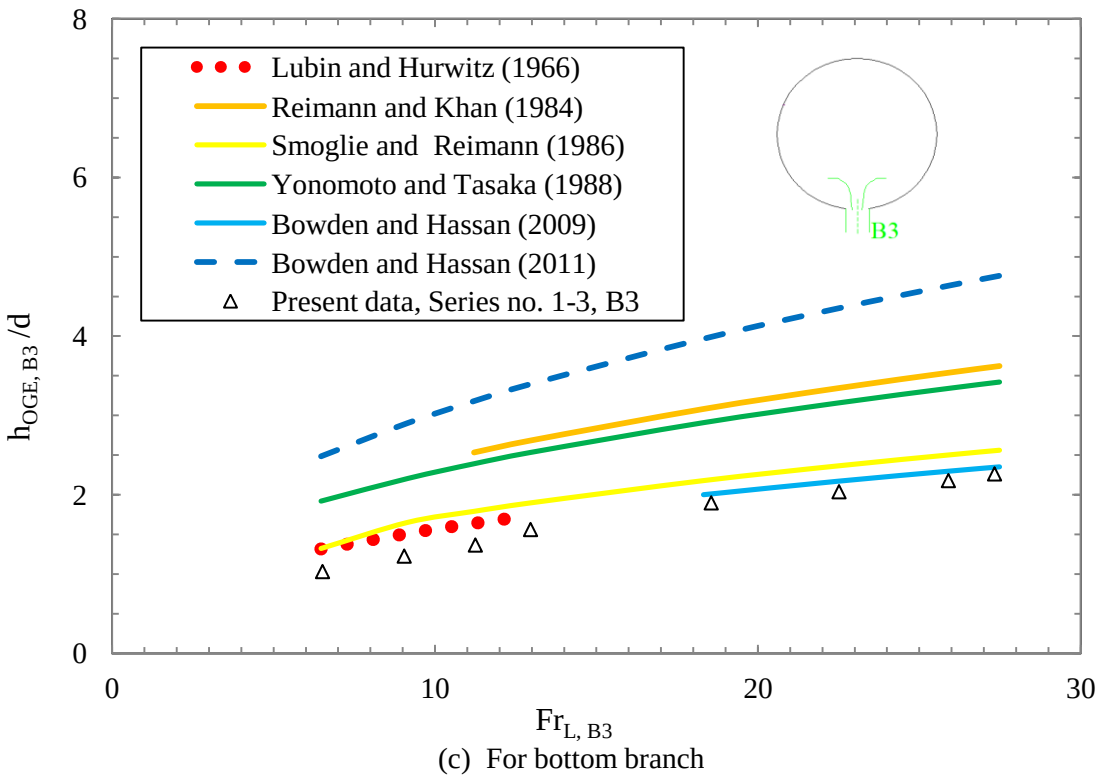

(c) For bottom branch

Figure 4.4 : Comparison of present data with existing correlations of single discharge (cont.)

Table 4.4: Comparison of present data with existing correlations of single discharge

Correlation	Mounting surface of the branch	Investigators	RMSD of experimental results (%)		
			For side branches	For inclined branch	For bottom branches
Empirical	Circular wall	Bowden and Hassan (2011)	X	-190.6	-121.8
		Riemann and Khan (1984)	X	X	-68.3
		Smoglie and Reimann (1986)	-22.3	X	-21.8
	Flat wall	Bartley et al. (2008)	±4.1	X	X
		Bowden and Hassan (2009)	X	X	-5.4
		Hassan et al. (1998)	±3.4	X	X
		Lubin and Hurwitz (1966)	X	X	-10.8
		Parrot et al. (1991)	-31.5	X	X
		Yonomoto and Tasaka (1988)	-22.3	X	-64.5
Semi-empirical	Circular wall	Lee et al. (2007)	-22.3	X	X
Theoretical	Flat wall	Ahmed et al. (2003)	-12.4	X	X
		Guyot et al. (2014)	-11.1	X	X

The major disagreements with the existing correlations are discussed below;

(1) For bottom branch, comparison between the present data with Riemann and Khan (1986) and Yonomoto and Tasaka (1988) shows the deviation of -68.3 percentage and -64.5 percentage respectively. The reason for the disagreement may be attributed to the imposed flow of liquid perpendicular to the bottom branch in their test chamber, whereas in the present study the liquid beyond the branch is stagnant.

(2) Comparison of present data of inclined and bottom branches with correlation of Bowden and Hassan (2011) shows the deviation of -190.6 percentage and -121.8 percentage. This deviation may be attributed to their test section condition of wavy flow or slug flow instead of stratified flow during their experiments, whereas present investigations were carried out with smooth stratified gas-liquid interface levels.

(3) From the present study, (Equations 4.1 and 4.3) showed the trend of increase of C_1 from the side branch to the bottom branch, whereas, Smoglie and Reimann (1986) showed contradictory trend. This may be due to the velocity of flow perpendicular to the branch flow in the test chamber during the experiments conducted by them, whereas in the present investigations, smooth stratified and stagnant gas-liquid levels were maintained in the test chamber.

4.5 Dual Discharge Experiments

Dual discharge experiments were conducted for ten combinations of branches. Two branches were opened simultaneously and results of each combination of branches for series nos. 2-1 to 2-10 were plotted for $\frac{h_{OGE}}{d}$ within the range for Fr_L. The present results were plotted and compared with the previous investigations of Parrott et al. (1991) for upper branch, Hassan et al. (1996a) for upper and lower branches, and Hassan et al. (1996b) for two side branches. New empirical correlations of the upper branch, lower branch, two side branches, and two inclined branches were developed for different branch combinations of dual discharge.

4.5.1 Presentation of data and correlations

Table 4.5 depicts the cases geometrically identical and unique branch combinations of dual discharge. Figure 4.5 shows the results for the $\frac{h_{OGE}}{d}$ for the dual discharge experiment for ten combinations of the branches. Empirical correlations for critical height were developed for different branch combinations and are given below.

Case no. 2-A: Activated side branch and inclined branch mounted below the side branch of series nos. 2-1 and 2-10.

(I) For side branches, i.e. B1 and B5;

$$\frac{h_{OGE}}{d} = 0.617\ Fr_L^{0.4} \tag{4.5}$$

(II) For inclined branches, i.e. B2 and B4;

$$\frac{h_{OGE}}{d} = 0.523\ Fr_L^{0.4} \tag{4.6}$$

Table 4.5: Cases of geometrically identical and unique branch combinations of dual discharge

Case no.	Series no.	Branch combinations			
		Upper Branch/es (UB)		Lower Branch (LB)	
		UB-1	UB-2 (opposite to UB-1)	LB-1	LB-2 (opposite to UB-1)
2-A	2-1	B1	X	B2	X
	2-10	B5	X	B4	X
2-B	2-2	B1	X	B3	X
	2-9	B5	X	B3	X
2-C	2-3	B1	X	X	B4
	2-7	B5	X	X	B2
2-D	2-4	B1	B5	X	X
2-E	2-5	B2	X	B3	X
	2-8	B4	X	B3	X
2-F	2-6	B2	B4	X	X

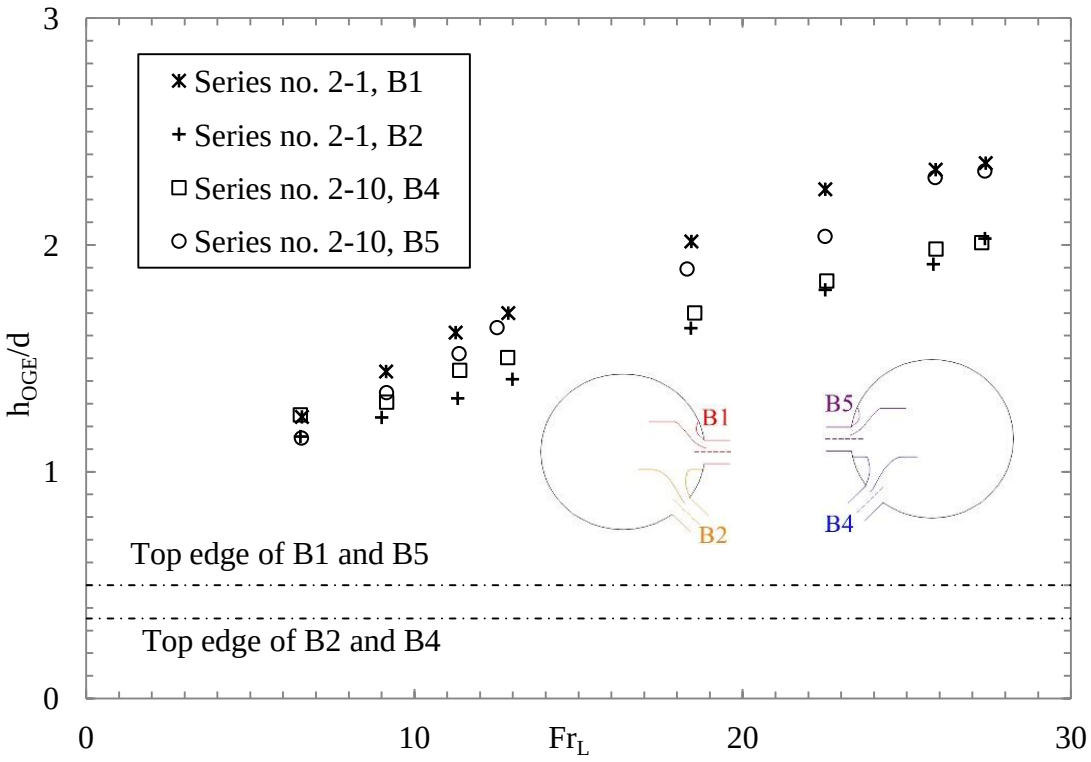

(a) Case no. 2-A

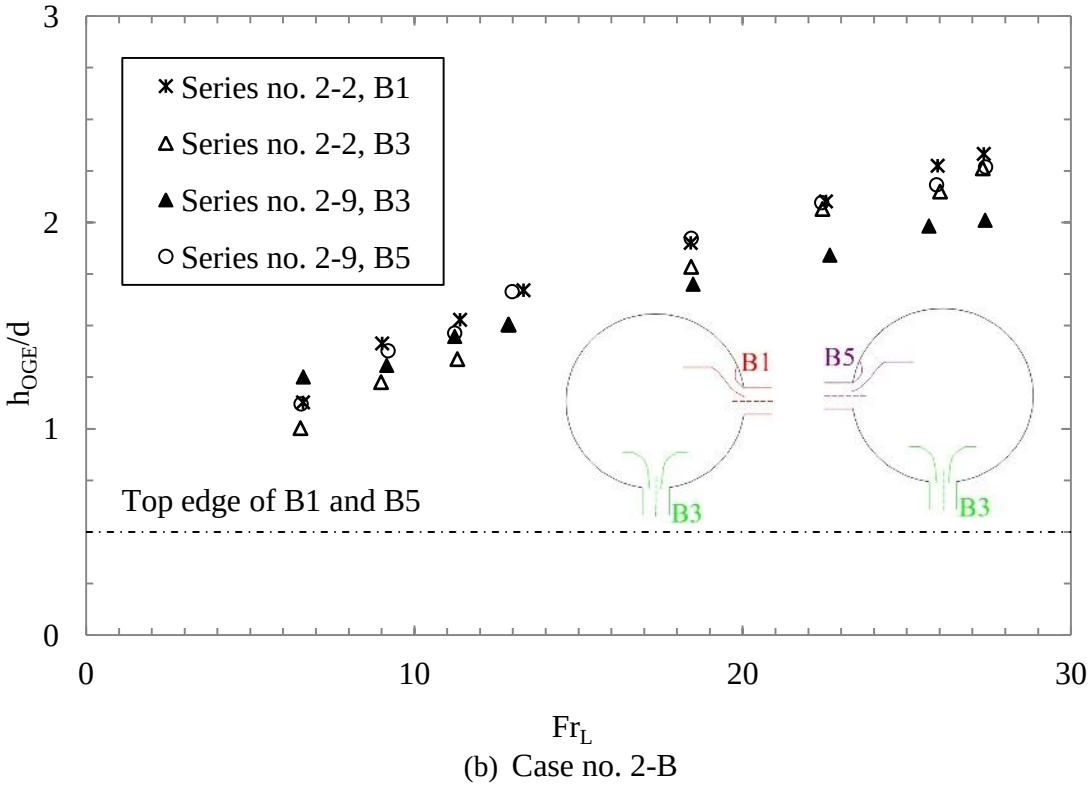

(b) Case no. 2-B

Figure 4.5: Interface level at the OGE of dual discharge experiment

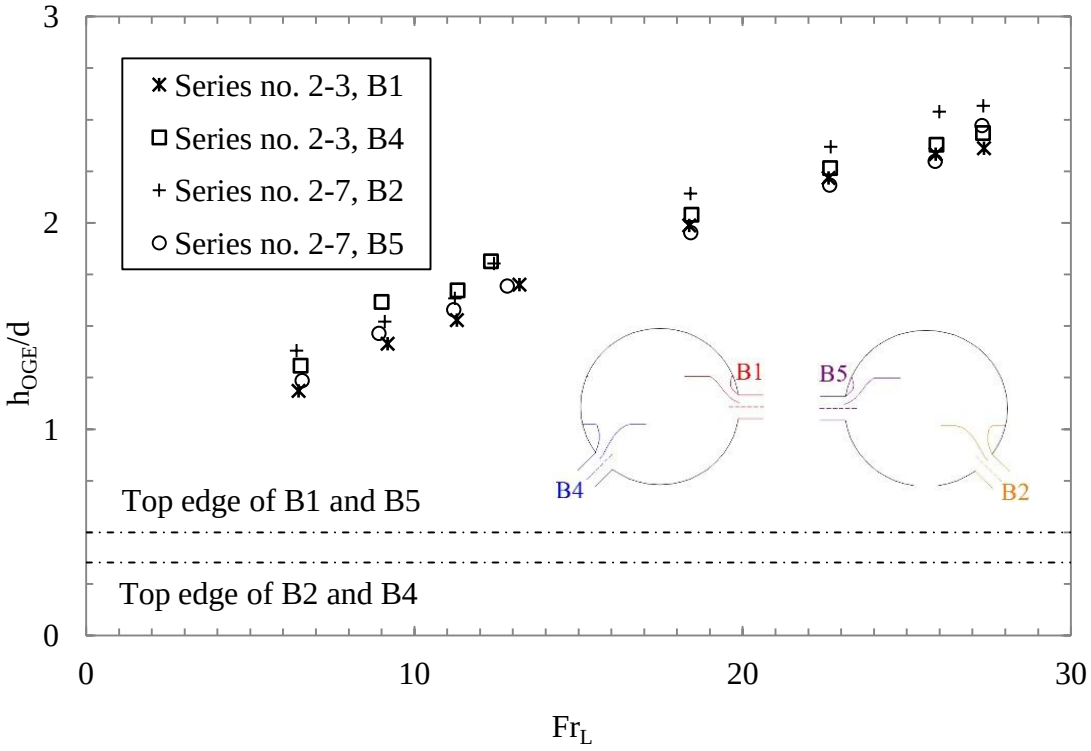

(c) Case no 2-C

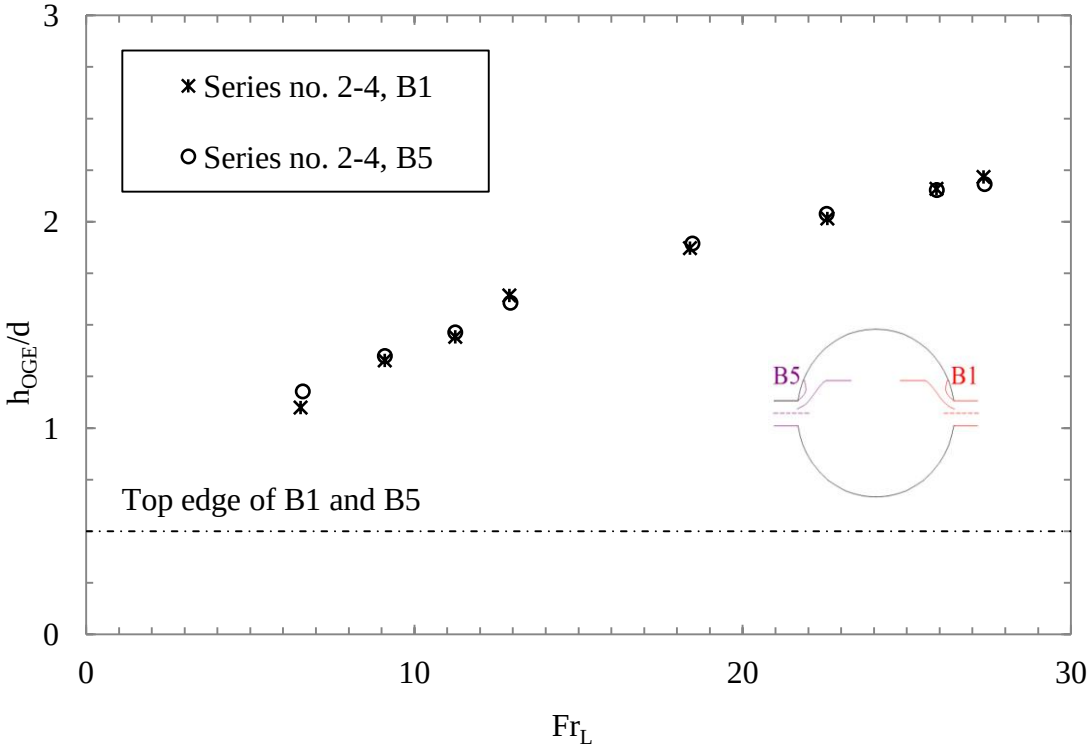

(d) Case no. 2-D

Figure 4.5: Interface level at the OGE of dual discharge experiment (cont.)

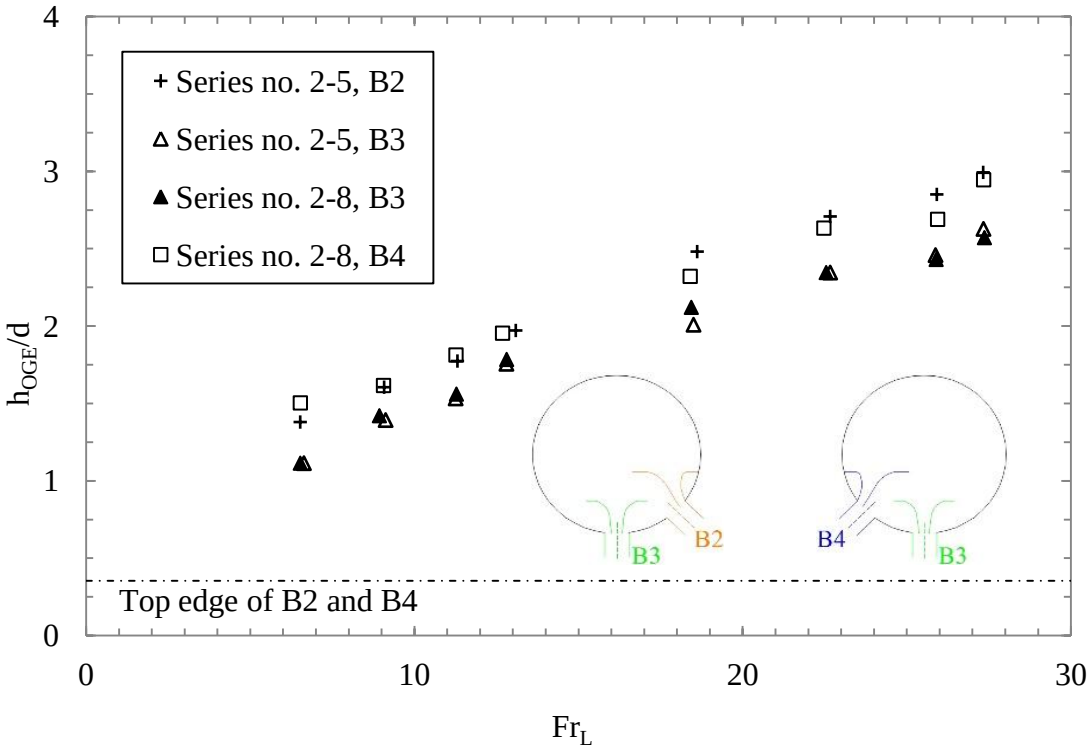

(e) Case no. 2-F

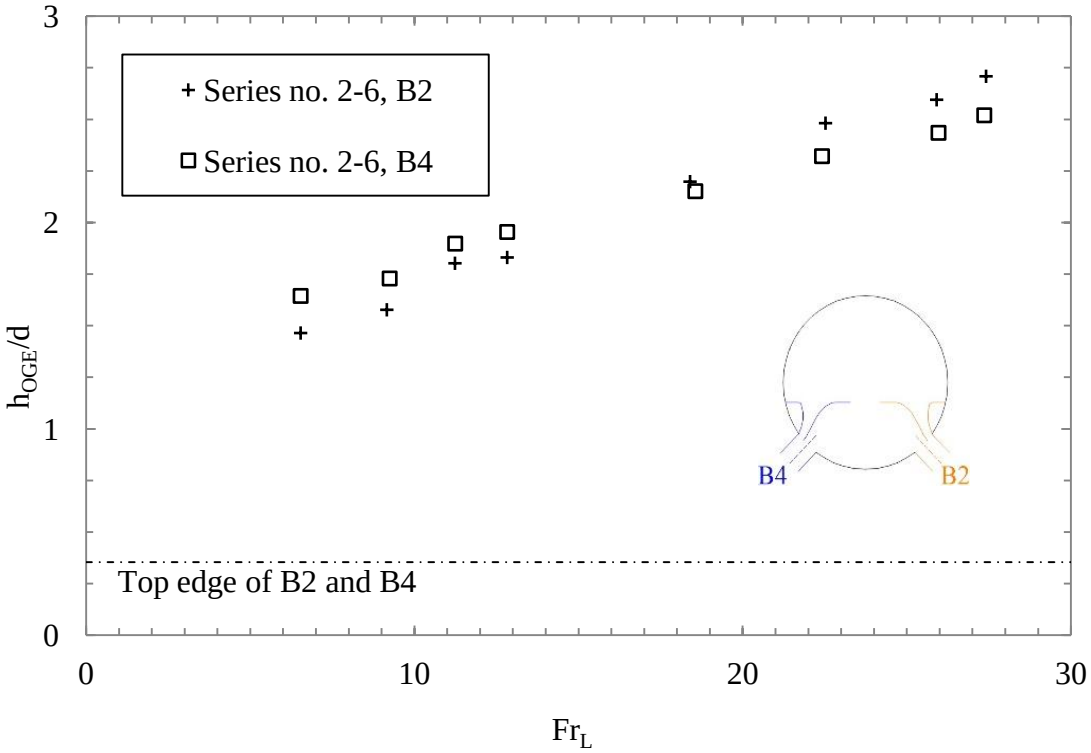

(f) Case no. 2-F

Figure 4.5: Interface level at the OGE of dual discharge experiment (cont.)

Case no. 2-B: Activated side branch and a bottom branch of series nos. 2-2 and 2-9.

(I) For side branches, i.e. B1 and B5;

$$\frac{h_{OGE}}{d} = 0.582\ Fr_L^{0.4} \tag{4.7}$$

(II) For bottom branch, i.e. B3;

$$\frac{h_{OGE}}{d} = 0.557\ Fr_L^{0.4} \tag{4.8}$$

Case no. 2-C: Activated side branch and inclined branch mounted opposite to the side branch of series nos. 2-3 and 2-7.

(I) For side branches, i.e. B1 and B5;

$$\frac{h_{OGE}}{d} = 0.617\ Fr_L^{0.4} \tag{4.9}$$

(II) For inclined branches mounted opposite to the side branch, i.e. B4 and B2;

$$\frac{h_{OGE}}{d} = 0.641\ Fr_L^{0.4} \tag{4.10}$$

Case no. 2 -D: Activated side branches mounted opposite to each other i.e. B1 and B5 of series no. 2-4.

$$\frac{h_{OGE}}{d} = 0.582\ Fr_L^{0.4} \tag{4.11}$$

Case no. 2-E: Activated inclined branch and a bottom branch of series nos. 2-5 and 2-8.

(I) For inclined branches, i.e. B2 and B4;

$$\frac{h_{OGE}}{d} = 0.730\ Fr_L^{0.4} \tag{4.12}$$

(II) For bottom branch, i.e. B3;

$$\frac{h_{OGE}}{d} = 0.641\ Fr_L^{0.4} \tag{4.13}$$

Case no. 2-F: Activated inclined branches mounted opposite to each other i.e. B2 and B4 of series no. 2-6.

$$\frac{h_{OGE}}{d} = 0.691\ Fr_L^{0.4} \tag{4.14}$$

For the case nos. 2-A, 2-B, 2-C, 2-D, 2-E and 2-F the RMSD is given in Table 4.6, when comparing the correlation and experimental $\frac{h_{OGE}}{d}$ over the range of branch Froude number.

To explore the effect of dual discharge condition on h_{OGE} the C_1 values of Table 4.3 of single discharge and Table 4.6 of dual discharge are compared. The higher C_1 value results into higher h_{OGE} and lower C_1 value results into lower h_{OGE} for the same Froude number.

Case no. 2-A shows that discharge from the lower branch increased C_1 of the upper branch compared to single discharge case no. 1-A. The discharge from the lower branch pulled the liquid around upper branch resulting in the gas entering easily into upper branch. Therefore, the discharge from lower branch supported early gas entrainment into upper branch. Case nos. 2-B, 2-C, and 2-E confirm the above effect for the discharges from upper branches.

Table 4.6: Correlation constants and RMSD for dual discharge

Case no.	Series no.	Branch combinations				Correlation constants					RMSD (%)			
		Upper Branch/es (UB)		Lower Branch (LB)		C_1				C_2				
		UB-1	UB-2 (opposite to UB-1)	LB-1 (below UB-1)	LB-2 (opposite to UB-1)	UB-1	UB-2	LB-1	LB-2		UB-1	UB-2	LB-1	LB-2
2-A	2-1 and 2-10	Side	X	Inclined	X	0.617	X	0.523	X	0.4	±6.3	X	±3.6	X
2-B	2-2 and 2-9		X	Bottom	X	0.582	X	0.557	X	0.4	±6.0	X	±7.2	X
2-C	2-3 and 2-7		X	X	Inclined	0.617	X	X	0.641	0.4	±6.3	X	X	±7.9
2-D	2-4 only		Side	X	X	0.582	0.582	X	X	0.4	±6.0	±6.0	X	X
2-E	2-5 and 2-8	Inclined	X	Bottom	X	0.730	X	0.641	X	0.4	±7.9	X	±7.9	X
2-F	2-6 only		Inclined	X	X	0.691	0.691	X	X	0.4	±7.0	±7.0	X	X

The effect of the discharges from two side branches (case no. 2-D) resulted in increased C_1 of both the side branches compared to single discharge case no. 1-A. The discharges from the two inclined branches (case no. 2-F) confirm the above effect. However, the effect was more significant for the two inclined branches compared to two side branches.

4.5.2 Comparison of present data with existing correlations

Figure 4.6 compares the present results with correlations for the branches mounted on vertical wall, as no correlations are available in open literature for the branches mounted on circular surface. The correlations proposed by Parrott et al. (1991) equation (2.10) for upper branch, Hassan et al. (1996a) equations (2.13) and (2.14) for upper and lower branches, and Hassan et al. (1996b) equation (2.17) for two opposite branches were used for comparison. The experimental results of upper branches are in good agreement with Hassan et al. (1996a) with the deviation between +7.7 percentage to +9.9 percentage. Comparison of present $\frac{h_{OGE}}{d}$ data of lower branch with the Hassan et al. (1996a) resulted in deviation between ±15.9 percentage and +47.6 percentage. This significant deviation may be because the different mounting surface of the branches, they used vertical wall for the mounting of the lower branch, whereas, in present study the lower branches were mounted on the circular surface. The experimental data of two side branches are in good agreement with the Hassan et al. (1996b) with the deviation of ±3.7 percentage, whereas the experimental data of two inclined branches resulted in deviation of +17.9 percentage. The two inclined branches being closer to each other could influence the discharges; therefore, the deviation was more compared to two side branches. Table 4.7 depicts a comparison of present results of dual discharge with existing correlations available in open literature.

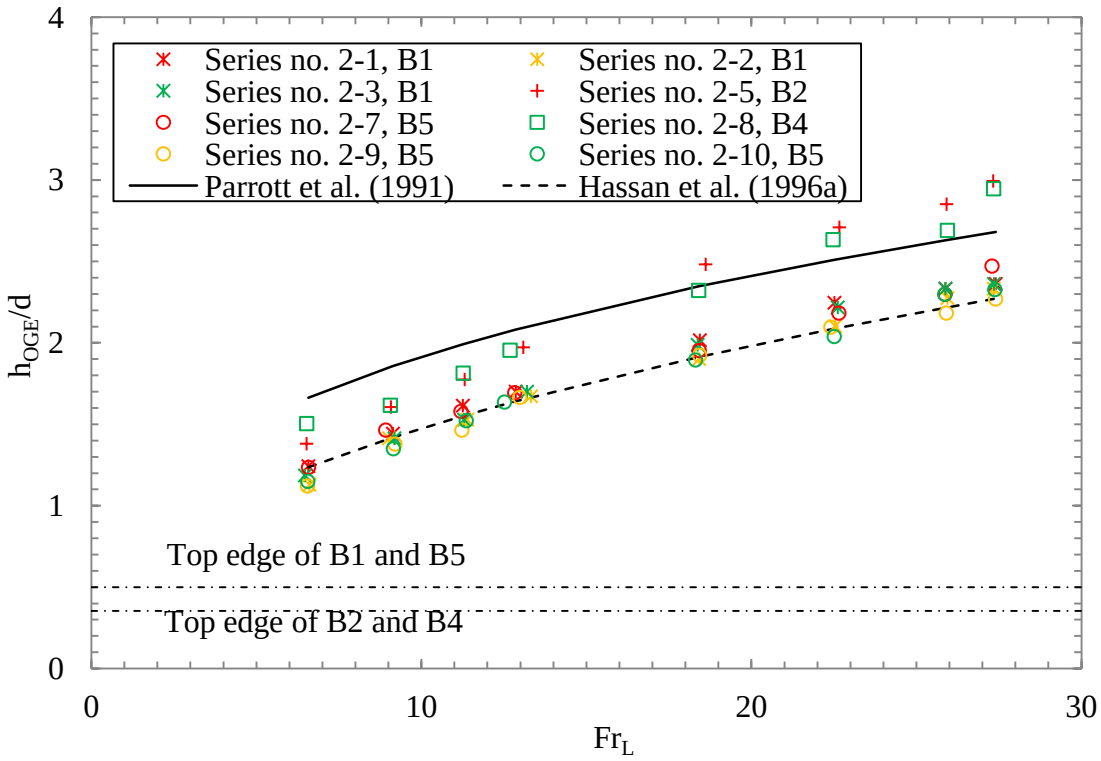

(a) For upper branch

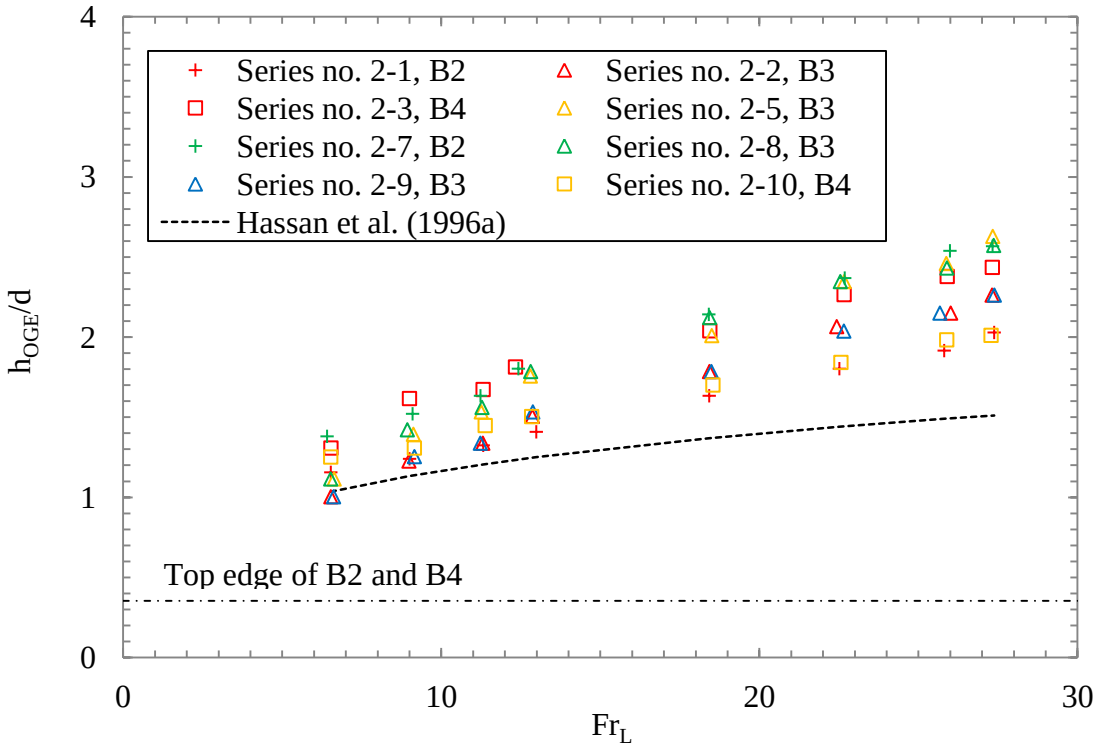

(b) For lower branch

Figure 4.6: Comparison of present data with existing correlations of dual discharge

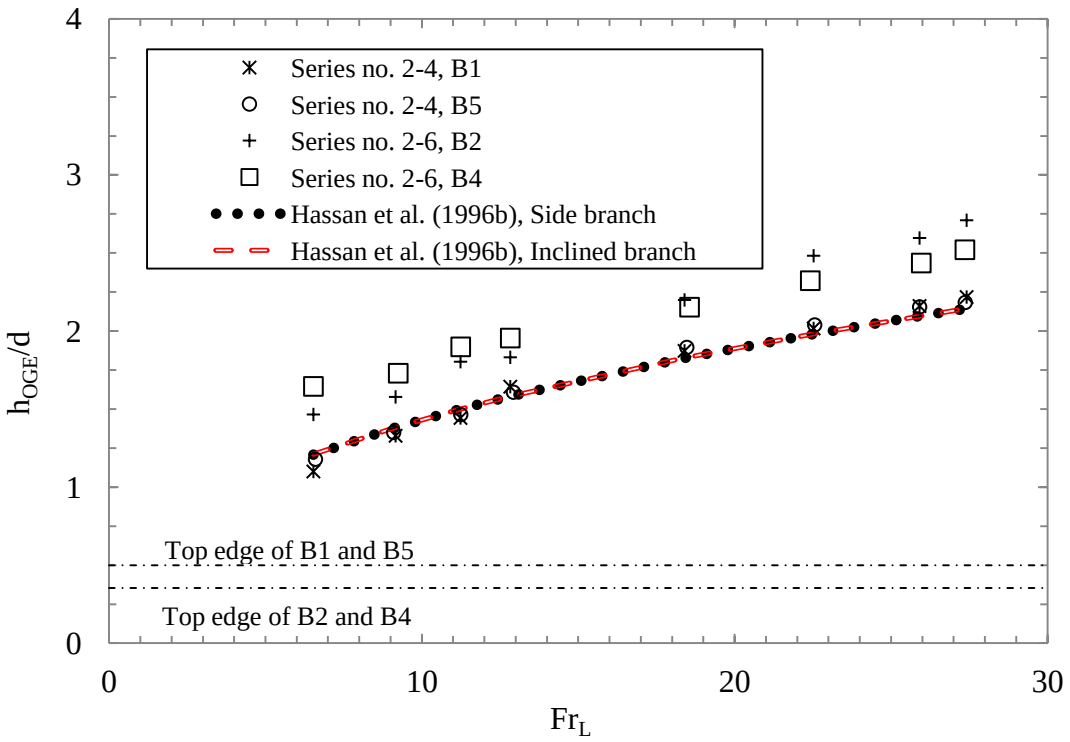

(c) For two opposite branches

Figure 4.6: Comparison of present data with existing correlations of dual discharge (cont.)

Table 4.7: Comparison of present data with existing correlations of dual discharge

Case no.	Investigator/s	Orientation of branches				L/d ratio	RMSD for experimental results (%)			
		Upper Branch/es (UB)		Lower Branch (LB)			UB-1	UB-2	LB-1	LB-2
		UB-1	UB-2 (opposite to UB-1)	LB-1 (below UB-1)	LB-2 (opposite UB-1)					
2-A	Parrot et al. (1991)	Side	X	Inclined	X	2.31	-30.1	X	X	X
	Hassan et al. (1996a)		X	Inclined	X	2.31	+8.0	X	+21.9	X
2-B	Parrot et al. (1991)		X	Bottom	X	3.26	-34.5	X	X	X
	Hassan et al. (1996a)		X	Bottom	X	3.26	+7.8	X	±15.9	X
2-C	Parrot et al. (1991)		X	X	Inclined	2.31	-20.3	X	X	X
	Hassan et al. (1996a)		X	X	Inclined	2.31	+7.7	X	X	+30.8
2-D	Hassan et al. (1996b)		Side	X	X	6.52	±3.7	±3.7	X	X
2-E	Parrot et al. (1991)	Inclined	X	Bottom	X	0.96	±19.1	X	X	X
	Hassan et al. (1996a)		X	Bottom	X	0.96	+9.9	X	+47.6	X
2-F	Hassan et al. (1996b)		Inclined	X	X	4.61	+17.9	+17.9	X	X

4.6 Triple Discharge Experiments

Triple discharge experiments were conducted for ten combinations of the branches. Three branches were opened simultaneously and results of each combination of branches for series nos. 3-1 to 3-10 were plotted for $\frac{h_{OGE}}{d}$ within the range of Fr_L. From the comprehensive review of the earlier investigations reported in open literature, it was found that studies on OGE for triple discharges are not available. New empirical correlations were developed based on the results of the present experiments.

4.6.1 Presentation of data and correlations

Table 4.8 shows the cases of geometrically identical and unique branch combinations for triple discharges. Figure 4.7 shows the results for the $\frac{h_{OGE}}{d}$ for the triple discharge experiments. Empirical correlations were developed for critical height of each branch during a triple discharge condition. They consist of following relations:

Case no. 3-A: Activated side branch, inclined branch mounted below the side branch, and a bottom branch (series nos. 3-1 and 3-10).

(I) For side branches, i.e. B1 and B5, inclined branches, i.e. B2 and B4, and bottom branch i.e. B3;

$$\frac{h_{OGE}}{d} = 0.641\ Fr_L^{0.4} \tag{4.15}$$

Case no. 3-B: Activated side branch, inclined branch mounted below the side branch, and an inclined branch mounted opposite to the side branch of series nos. 3-2 and 3-9.

Table 4.8: Cases of geometrically identical and unique branch combinations of triple discharge

Case no.	Series no.	Branch combinations					
		Upper Branch/es (UB)		Middle Branch (MB)		Lower Branch/es (LB)	
		UB-1	UB-2 (opposite to UB-1)	MB-1 (below UB-1)	MB-2 (opposite to UB-1)	LB-1 (below UB-1)	LB-2 (opposite to UB-1)
3-A	3-1	B1	X	B2	X	B3	X
	3-10	B5	X	B4	X	B3	X
3-B	3-2	B1	X	X	X	B2	B4
	3-9	B5	X	X	X	B4	B2
3-C	3-3	B1	B5	X	X	B2	X
	3-6	B5	B1	X	X	B4	X
3-D	3-4	B1	X	X	B4	X	B3
	3-8	B5	X	X	B2	X	B3
3-E	3-5	B1	B5	X	X	X	B3
3-F	3-7	B2	B4	X	X	X	B3

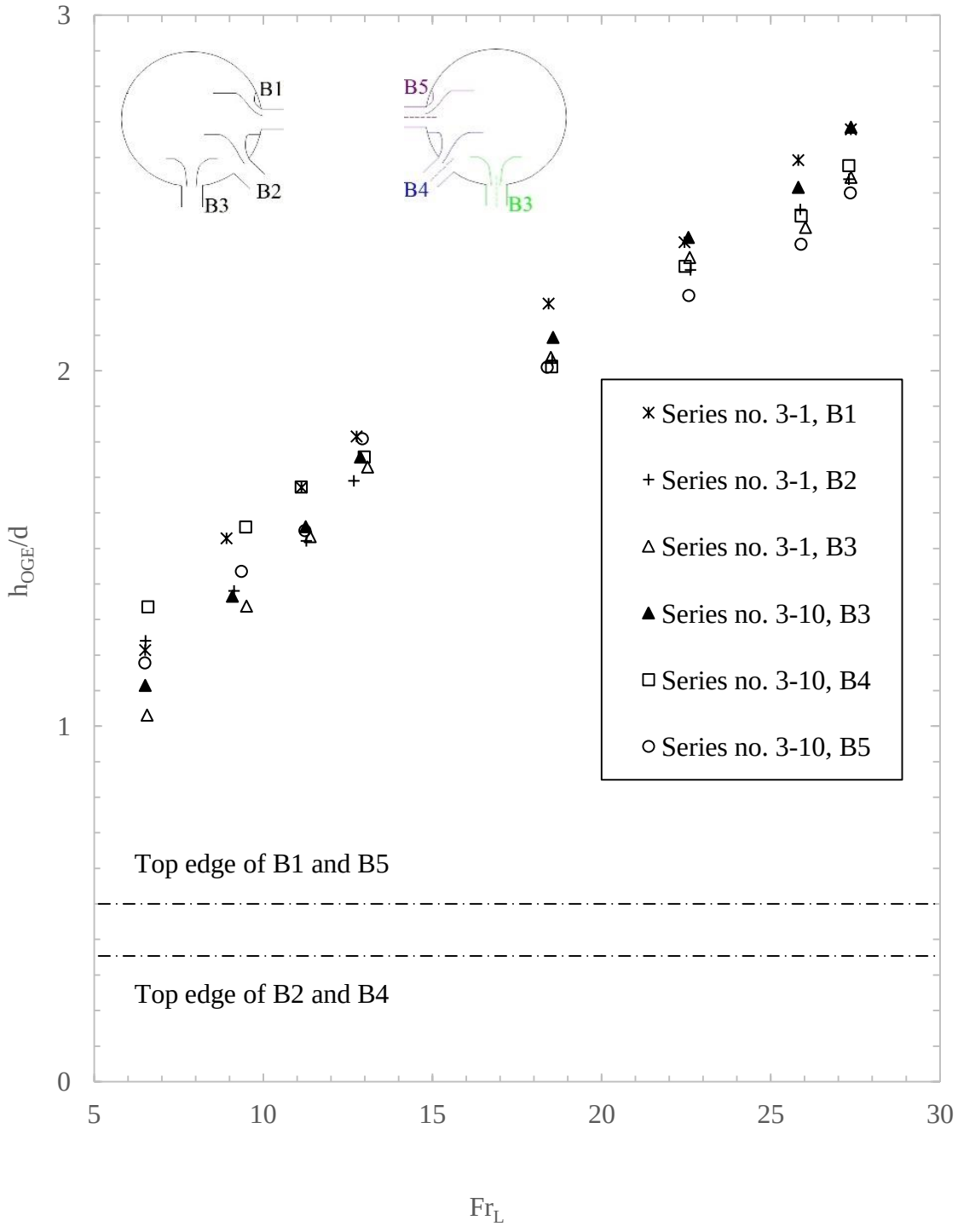

(a) Case no. 3-A

Figure 4.7: Interface level at the OGE of triple discharge experiment

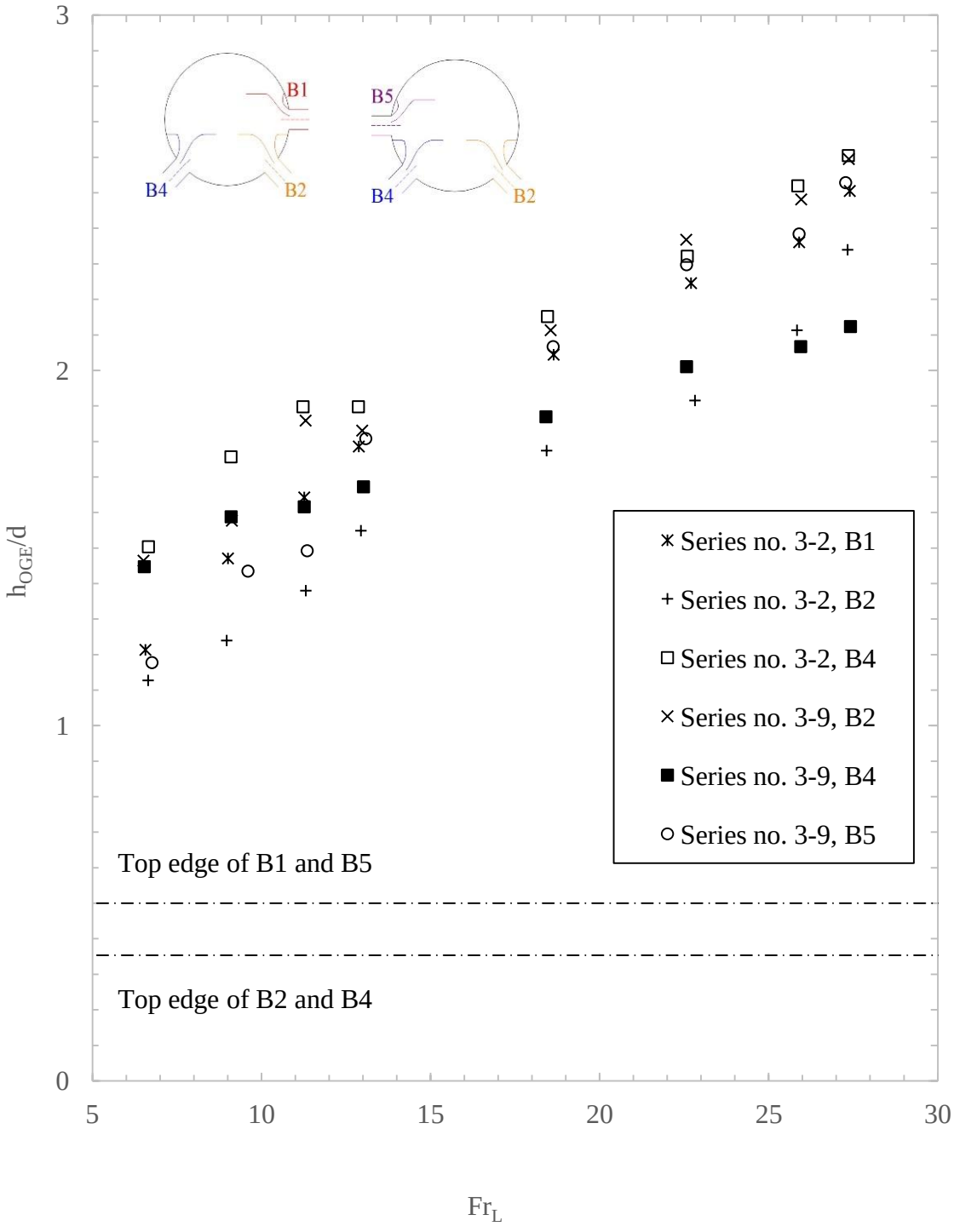

(b) Case no. 3-B

Figure 4.7: Interface level at the OGE of triple discharge experiment (cont.)

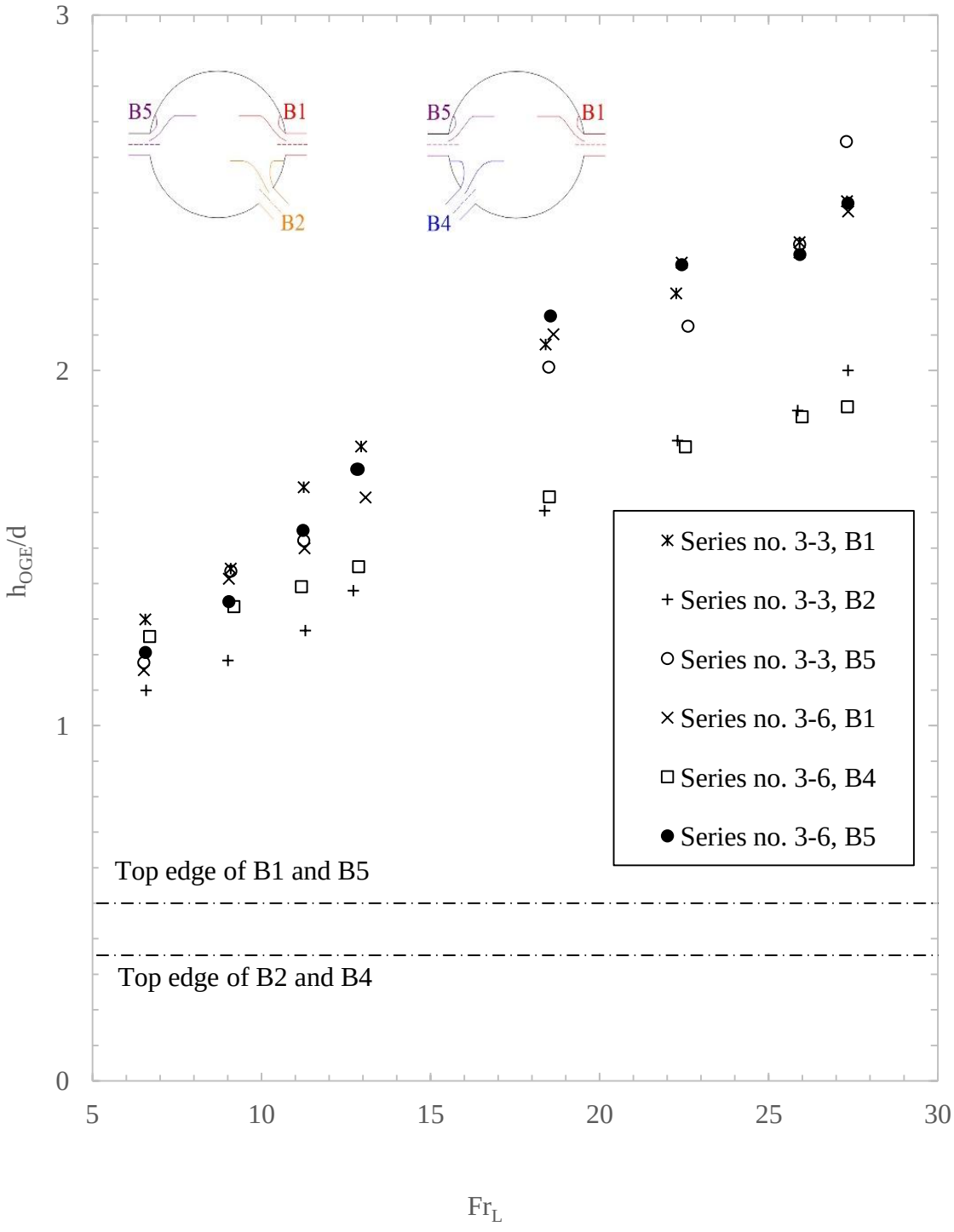

(c) Case no. 3-C

Figure 4.7: Interface level at the OGE of triple discharge experiment (cont.)

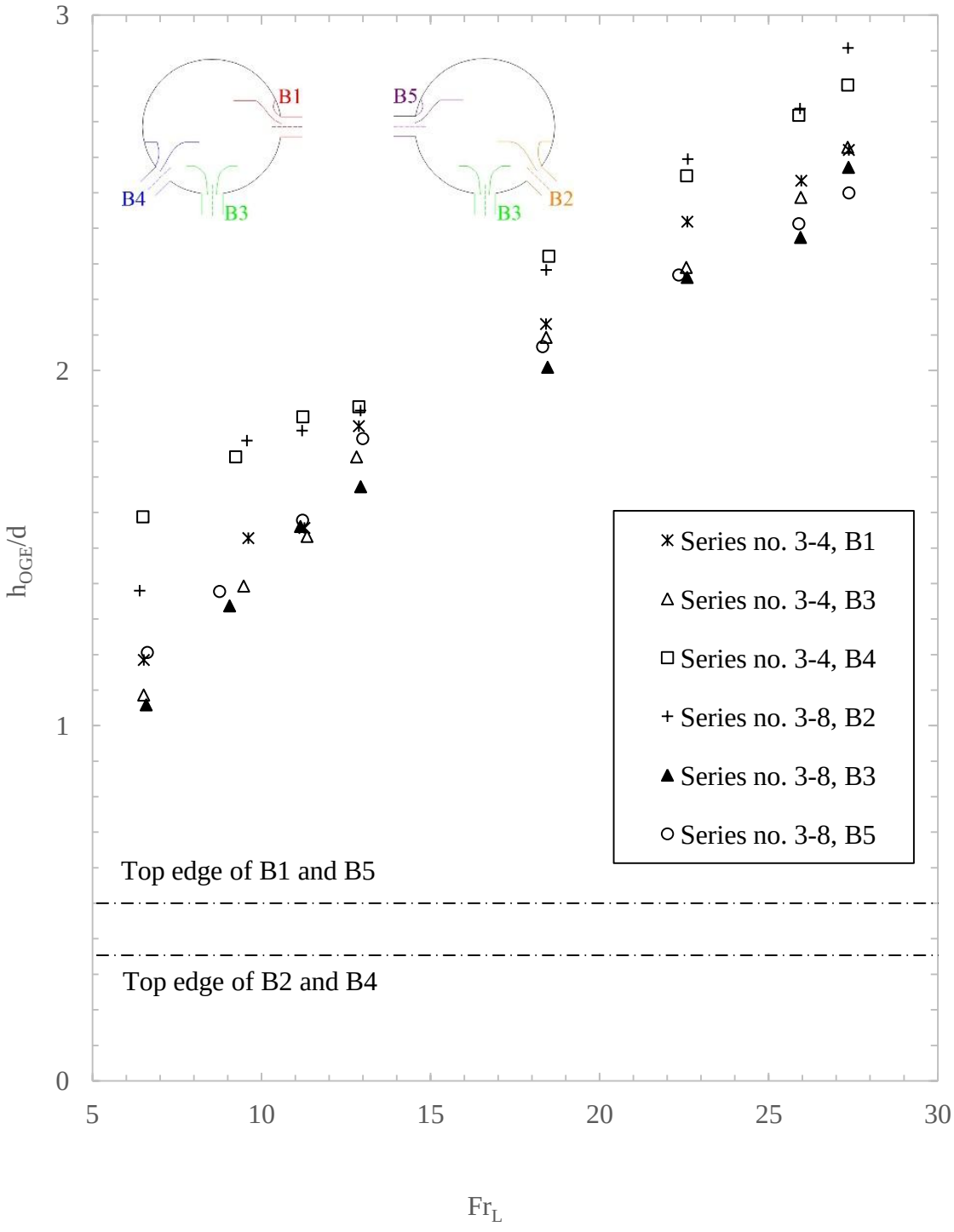

(d) Case no. 3-D

Figure 4.7: Interface level at the OGE of triple discharge experiment (cont.)

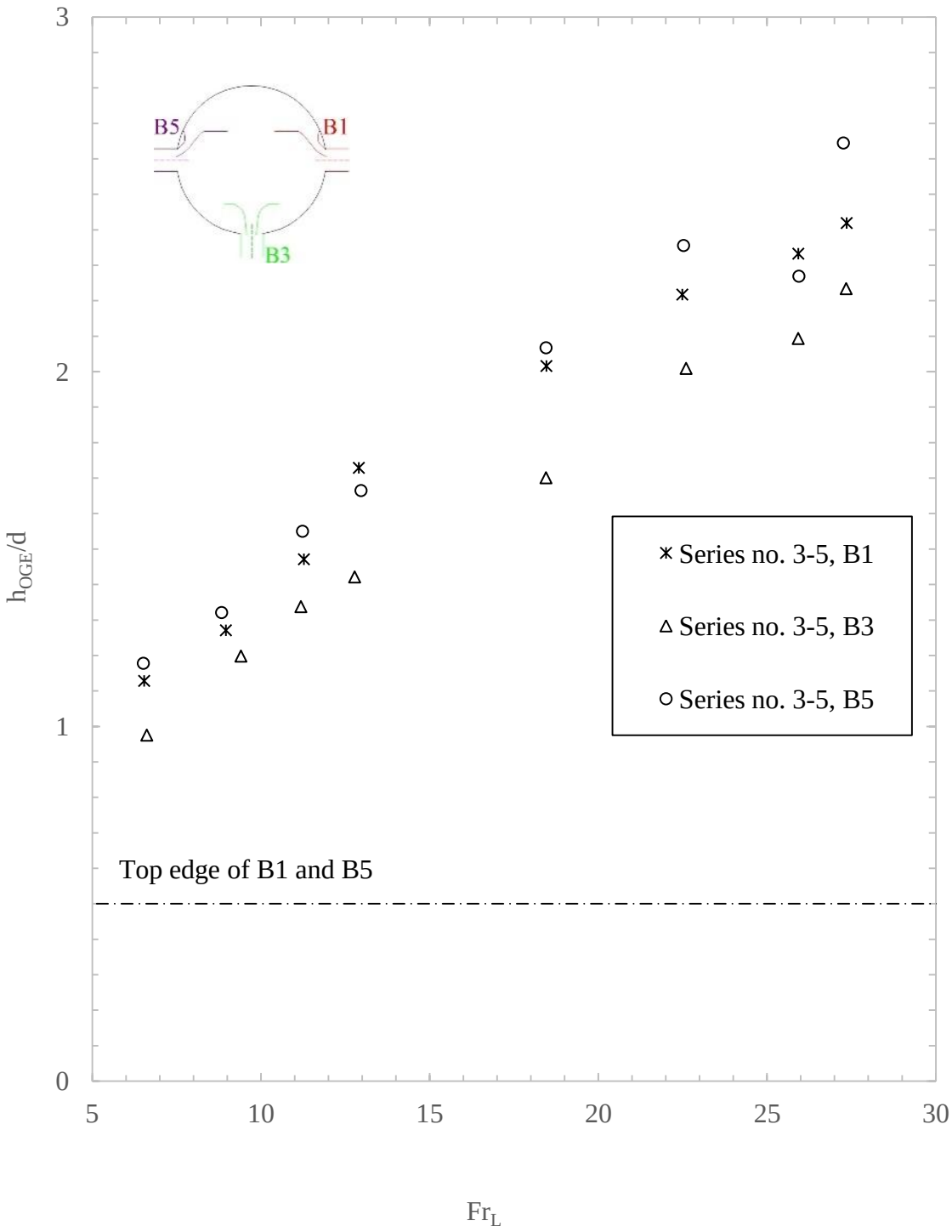

(e) Case no. 3-E

Figure 4.7: Interface level at the OGE of triple discharge experiment (cont.)

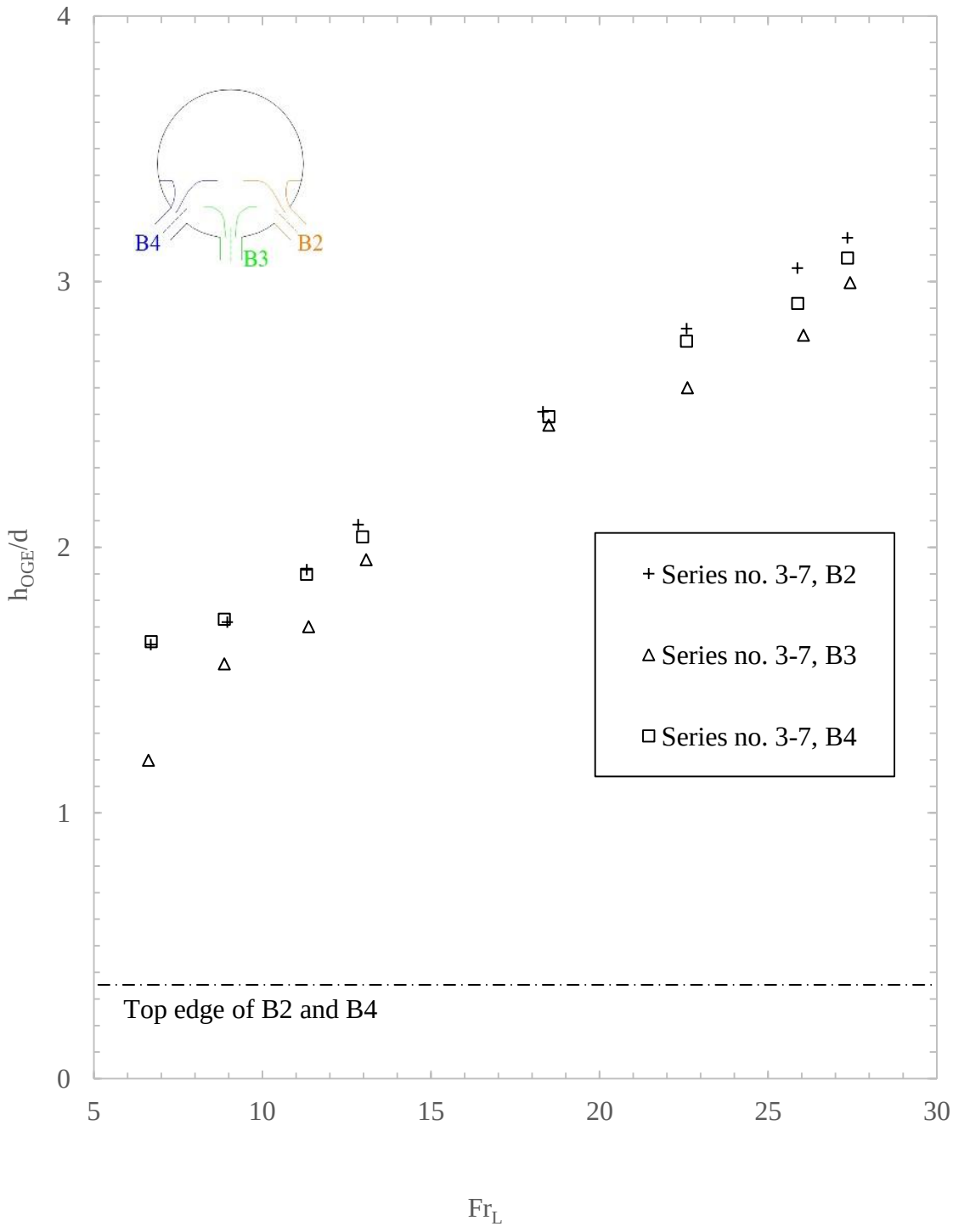

(f) Case no. 3-F

Figure 4.7 Interface level at the OGE of triple discharge experiment (cont.)

(I) For side branches, i.e. B1 and B5;

$$\frac{h_{OGE}}{d} = 0.641\ Fr_L^{0.4} \tag{4.16}$$

(II) For inclined branches mounted below the side branch, i.e. B2 and B4;

$$\frac{h_{OGE}}{d} = 0.582\ Fr_L^{0.4} \tag{4.17}$$

(III) For inclined branches mounted opposite to the side branch, i.e. B4 and B2;

$$\frac{h_{OGE}}{d} = 0.691\ Fr_L^{0.4} \tag{4.18}$$

Case no. 3-C: Activated two side branches, and inclined branch mounted opposite to the side branch of series nos. 3-3 and 3-6.

(I) For side branches, i.e. B1 and B5;

$$\frac{h_{OGE}}{d} = 0.641\ Fr_L^{0.4} \tag{4.19}$$

(II) For inclined branches mounted opposite to the side branch, i.e. B4 and B2;

$$\frac{h_{OGE}}{d} = 0.523\ Fr_L^{0.4} \tag{4.20}$$

Case no. 3-D: Activated side branch, inclined branch mounted opposite to side branch, and a bottom branch of series nos. 3-4 and 3-8.

(I) For side branches, i.e. B1 and B5 and bottom branch i.e. B3;

$$\frac{h_{OGE}}{d} = 0.641\ Fr_L^{0.4} \tag{4.21}$$

(II) For inclined branches mounted opposite to the side branch, i.e. B4 and B2;

$$\frac{h_{OGE}}{d} = 0.730\ \ Fr_L^{0.4} \tag{4.22}$$

Case no. 3-E: Activated two side branches and a bottom branch of series no. 3-5.

(I) For side branches, i.e. B1 and B5;

$$\frac{h_{OGE}}{d} = 0.617\ Fr_L^{0.4} \tag{4.23}$$

(II) For bottom branch, i.e. B3;

$$\frac{h_{OGE}}{d} = 0.557\ Fr_L^{0.4} \tag{4.24}$$

Case no. 3-F: Activated two inclined branches and a bottom branch of series no. 3-7.

(I) For inclined branches, i.e. B2 and B4;

$$\frac{h_{OGE}}{d} = 0.794\ Fr_L^{0.4} \tag{4.25}$$

(II) For bottom branch, i.e. B3;

$$\frac{h_{OGE}}{d} = 0.730\ Fr_L^{0.4} \tag{4.26}$$

For the case nos. 3-A, 3-B, 3-C, 3-D, 3-E, and 3-F the RMSD is given in Table 4.9, when comparing the correlation and experimental values of $\frac{h_{OGE}}{d}$ over the range of branch Froude number.

C_1 for the branches during triple discharge experiments were mostly different from single discharges and dual discharges.

It is interesting to note that C_1 of the side-1, inclined-1, and bottom branches in case no. 3-A is same. The study of case nos. 2-A and 2-B showed that discharges from the side-1 branch decreased C_1 of the inclined-1 branch and the bottom branch. Therefore, it is expected that C_1 of inclined-1 and bottom branches should be lower than the side-1 branch. However, the study of simultaneous discharges from the inclined-1 branches and bottom branch (case no. 2-E) showed significant increase in

Table 4.9: Correlation constants and RMSD for triple discharge

Case no.	Series no.	Branch combinations						Correlation constants							RMSD (%)					
		Upper Branch/es (UB)		Middle Branch (MB)		Lower Branch/es (LB)		C1						C_2						
		UB-1	UB-2 (opposite to UB-1)	MB-1 (below UB-1)	MB-2 (opposite to UB-1)	LB-1 (below UB-1)	LB-2 (opposite to UB-1)	UB-1	UB-2	MB-1	MB-2	LB-1	LB-2		UB-1	UB-2	MB-1	MB-2	LB-1	LB-2
3-A	3-1 and 3-10	Side -1	X	Inclined -1	X	Bottom	X	0.641	X	0.641	X	0.641	X	0.4	±7.9	X	±7.9	X	±7.9	X
3-B	3-2 and 3-9		X	X	X	Inclined-1	Inclined-2	0.641	X	X	X	0.582	0.691	0.4	±7.9	X	X	X	±6.0	±7.0

Table 4.9: Correlation constants and RMSD for triple discharge (con

Case no.	Series no.	Branch combinations						Correlation constants							RMSD (%)					
		Upper Branch/es (UB)		Middle Branch (MB)		Lower Branch/es (LB)		C_1						C_2						
		UB-1	UB-2 (opposite to UB-1)	MB-1 (below UB-1)	MB-2 (opposite to UB-1)	LB-1 (below UB-1)	LB-2 (opposite to UB-1)	UB-1	UB-2	MB-1	MB-2	LB-1	LB-2		UB-1	UB-2	MB-1	MB-2	LB-1	LB-2
3-C	3-3 and 3-6	Side-1	Side -2	X	X	Inclined -1	X	0.641	0.641	X	X	0.523	X	0.4	±7.9	±7.9	X	X	±3.6	X
3-D	3-4 and 3-8		X	X	Inclined-1	Bottom	X	0.641	X	X	0.730	0.641	X	0.4	±7.9	X	X	±7.9	±7.9	X

Table 4.9: Correlation constants and RMSD for triple discharge (cont.)

Case no.	Series no.	Branch combinations						Correlation constants							RMSD (%)					
		Upper Branch/es (UB)		Middle Branch (MB)		Lower Branch/es (LB)		C_1						C_2						
		UB-1	UB-2 (opposite to UB-1)	MB-1 (below UB-1)	MB-2 (opposite to UB-1)	LB-1 (below UB-1)	LB-2 (opposite to UB-1)	UB-1	UB-2	MB-1	MB-2	LB-1	LB-2		UB-1	UB-2	MB-1	MB-2	LB-1	LB-2
3-E	3-5 only	Side-1	Side-2	X	X	Bottom	X	0.617	0.617	X	X	0.557	X	0.4	±6.3	±6.3	X	X	±7.2	X
3-F	3-7 only	Inclined-1	Inclined-2	X	X	Bottom	X	0.794	0.794	X	X	0.730	X	0.4	±6.7	±6.7	X	X	±7.9	X

C_1 of both the branches. As a result, simultaneous discharges from the inclined-1 and bottom branches surpassed the effect of discharges from the side-1 branch on them and C1 of both the branches increased compared to dual discharge (case nos. 2-A and 2-B).

The comparison of C_1 of case no. 3-B showed that discharge from the side-1 branch decreased C_1 of inclined-1 branch and increased C_1 of inclined-2 branch. Therefore, the effect of discharge from side-1 branch on C_1 of inclined branch was agreeing with case no. 2-A. The discharges from the side-1 and inclined-1 branches pulled liquid around the inclined-2 branch, therefore gas could easily enter it resulting in increased C_1 of inclined-2 branch.

The case no. 3-C showed the significant effect of the discharges from the two side branches on the inclined-1 branch; where C_1 of inclined-1 branch was lower than C_1 of side-1 branch. This was agreeing with the case no. 2-A.

In case no. 3-D, the discharges from side branch and bottom branch increased C_1 of the inclined-2 branch. This effect was agreeing with case nos. 2-C and 2-E.

C_1 of the bottom branch in case no. 3-E was significantly lowered by two simultaneous discharges from the side branches, because both the side branches pulled the gas around bottom branch. This effect is agreeing with the case no. 2-B.

On the other hand, the simultaneous discharges from the two inclined branches and bottom branch of case no. 3-F increased C_1 of the inclined branches and bottom branch. This effect agreeing with the case no. 2-E.

4.7 Quadruple Discharge Experiments

Quadruple discharge experiments were conducted for five combinations of the branches. Four branches were opened simultaneously and results of each combination of branches for series nos. 4-1 to 4-5 were plotted for $\frac{h_{OGE}}{d}$ within the range for Fr_L. The quadruple discharge condition has not previously been investigated. Empirical correlations were developed based on the results of the present experiments.

4.7.1 Presentation of data and correlations

Table 4.10 depicts the cases geometrically identical and unique branch combinations of quadruple discharge. Figure 4.8 shows the results for $\frac{h_{OGE}}{d}$ for the quadruple discharge experiment. Empirical correlations were developed for critical height of each branch during a quadruple discharge condition. They consist of following relations:

Case no. 4-A: Activated side branch, two inclined branches, and a bottom branch of series nos. 4-1 and 4-5.

(I) For side branches, i.e. B1 and B5;

$$\frac{h_{OGE}}{d} = 0.691\ Fr_L^{0.4} \tag{4.27}$$

(II) For inclined branches mounted below the side branch, i.e. B2 of series no. 4-1 and B4 of series no. 4-5;

$$\frac{h_{OGE}}{d} = 0.730\ Fr_L^{0.4} \tag{4.28}$$

Table 4.10: Cases of geometrically identical and unique branch combinations of quadruple discharge

Case no.	Series no.	Branch combinations					
		Upper Branch/es (UB)		Middle Branch/es (MB)		Lower Branch/es (LB)	
		UB-1	UB-2 (opposite to UB-1)	MB-1 (below UB-1)	MB-2 (opposite to UB-1)	LB-1 (below UB-1)	LB-2 (opposite to UB-1)
4-A	4-1	B1	X	B2	B4	B3	X
	4-5	B5	X	B4	B2	B3	X
4-B	4-2	B1	B5	X	B2	B3	X
	4-4	B5	B1	X	B4	B3	X
4-C	4-3	B1	B5	X	X	B2	B4

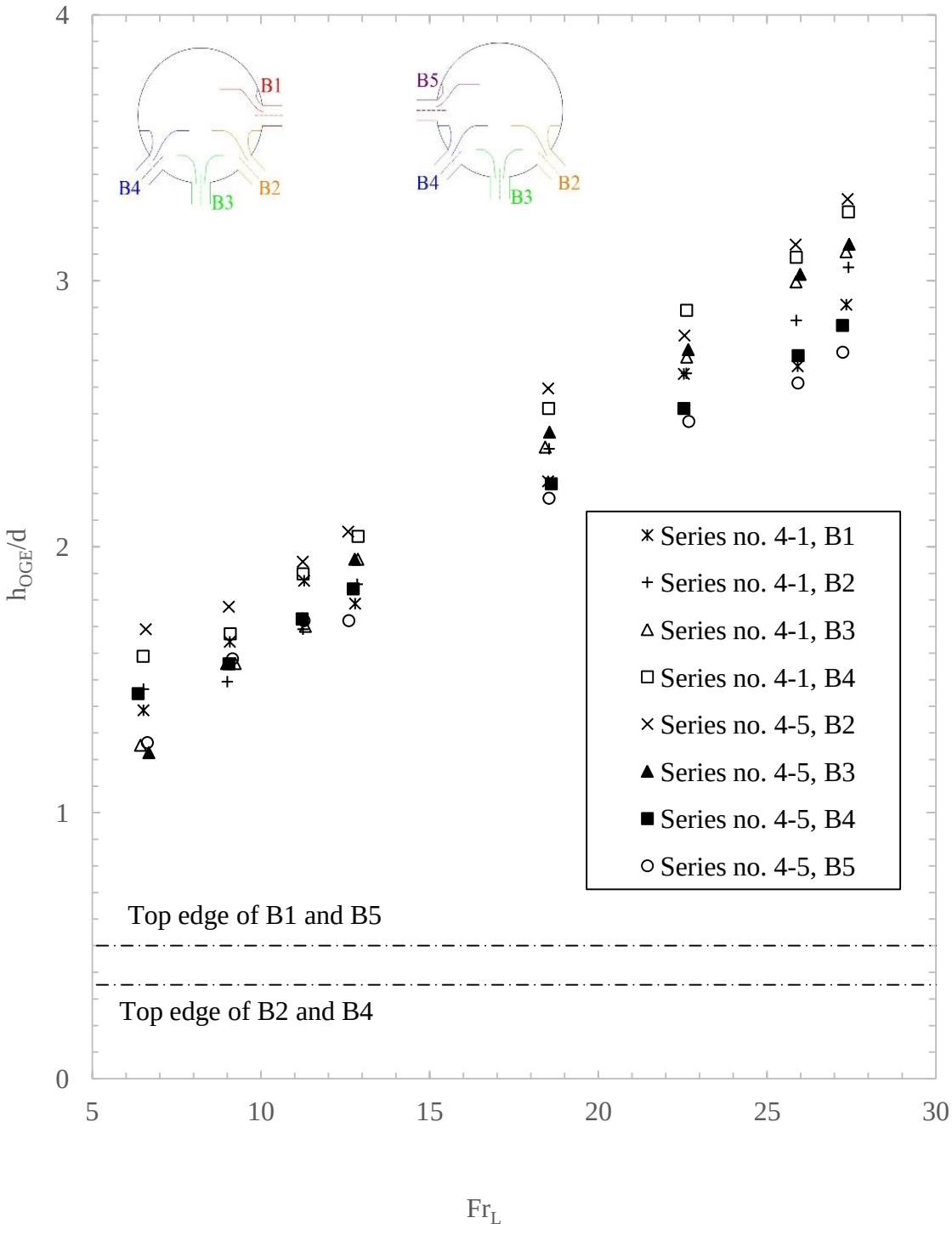

(a) Case no. 4-A

Figure 4.8: Interface level at the OGE of quadruple discharge experiment

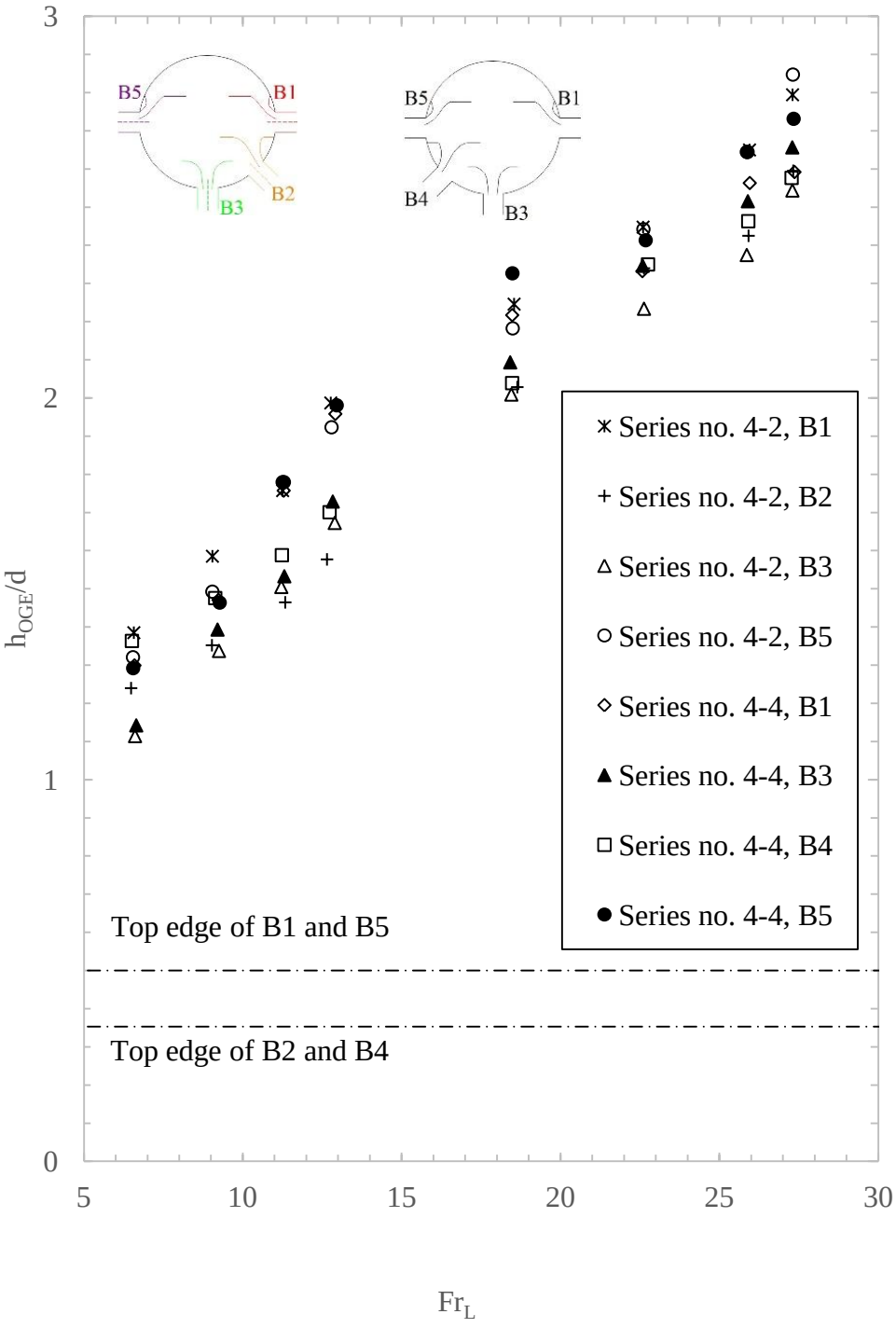

(b) Case no. 4-B

Figure 4.8: Interface level at the OGE of quadruple discharge experiment (cont.)

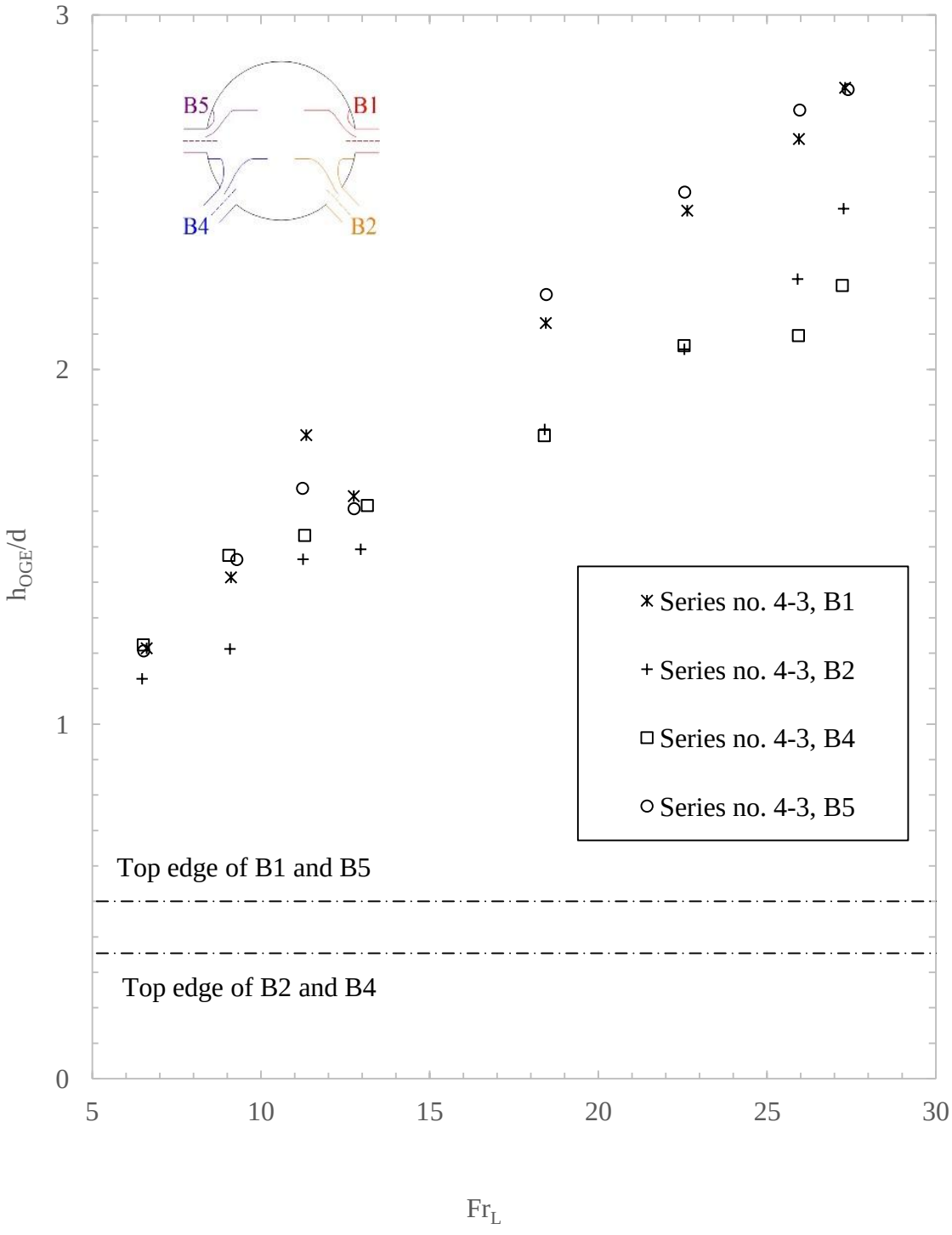

(c) Case no. 4-C

Figure 4.8: Interface level at the OGE of quadruple discharge experiment (cont.)

(III) For inclined branches mounted opposite to the side branch, i.e. B4 of series no. 4-1 and B2 of series no. 4-5;

$$\frac{h_{OGE}}{d} = 0.794\ Fr_L^{0.4} \tag{4.29}$$

(IV) For bottom branch, i.e. B3;

$$\frac{h_{OGE}}{d} = 0.750\ Fr_L^{0.4} \tag{4.30}$$

Case no. 4-B: Activated two side branches, an inclined branch mounted opposite to the side branch, and a bottom branch of series nos. 4-2 and 4-4.

(I) For side branches, i.e. B1 and B5;

$$\frac{h_{OGE}}{d} = 0.691\ Fr_L^{0.4} \tag{4.31}$$

(II) For inclined branches, i.e. B2 and B4 and bottom branch i.e. B3;

$$\frac{h_{OGE}}{d} = 0.641\ Fr_L^{0.4} \tag{4.32}$$

Case no. 4-C: Activated two side branches, two inclined branches of series no. 4-3.

(I) For two side branches, i.e. B1 and B5;

$$\frac{h_{OGE}}{d} = 0.691\ Fr_L^{0.4} \tag{4.33}$$

(II) For two inclined branches, i.e. B2 and B4;

$$\frac{h_{OGE}}{d} = 0.582\ Fr_L^{0.4} \tag{4.34}$$

For the case nos. 4-A, 4-B, and 4-C the RMSD is shown in Table 4.11, when comparing the correlation and experimental values of $\frac{h_{OGE}}{d}$ over the range of branch Froude number. It is clear from the table that C_1 for quadruple discharge experiments are mostly different from the single, dual, and triple discharge experiments.

Table 4.11: Correlation constants and RMSD for quadruple discharge

Case no.	Series no.	Branch combinations						Correlation constants							RMSD (%)					
		Upper Branch/es (UB)		Middle Branch/es (MB)		Lower Branch/es (LB)		C_1						C_2						
		UB-1	UB-2 (opposite to UB-1)	MB-1 (below UB-1)	MB-2 (opposite to UB-1)	LB-1 (below UB-1)	LB-2 (opposite to UB-1)	UB-1	UB-2	MB-1	MB-2	LB-1	LB-2		UB-1	UB-2	MB-1	MB-2	LB-1	LB-2
4-A	4-1 and 4-5	Side -1	X	Inclined -1	Inclined -2	Bottom	X	0.691	X	0.73	0.794	0.750	X	0.4	±7.0	X	±7.9	±6.7	±14.0	X
4-B	4-2 and 4-4		Side-2	Inclined -1	X	Bottom	X	0.691	0.691	0.641	X	0.641	X	0.4	±7.0	±7.0	±7.9	X	±7.9	X
4-C	4-3 only		Side -2	X	X	Inclined -1	Inclined-2	0.691	0.691	X	X	0.582	0.582	0.4	±7.0	±7.0	X	X	±6.0	±6.0

The case no. 4-A, showed that C_1 of inclined-1 branch was higher than the side-1 branch. This effect is, obviously, opposite to the case nos. 2-A and 3-B. However, the case nos. 2-E, 3-A, 3-B, 3-D, and 3-F showed that inclined and bottom branches increased the value of C_1 of both the branches significantly. As a result, simultaneous discharges from the two inclined branches and bottom branch surpassed the effect of discharge from side-1 branch and C_1 of inclined-1 branch was increased.

C_1 of inclined-1 and bottom braches were lower than two side branches as seen in case no. 4-B. This effect was agreeing with case nos. 3-C and 3-E.

C_1 of two side branches are higher than the two inclined branches in case no. 4-C. This effect was in agreement with case nos. 2-A, and 3-C.

4.8 Quintuple Discharge Experiments

Experiments conducted for one combination of the quintuple discharge. Five branches were made active simultaneously and results for series nos. 5-1 were plotted for $\frac{h_{OGE}}{d}$ within the range for Fr_L. The quintuple discharge condition has not previously been investigated. New empirical correlations were developed based on the results of the experiments.

4.8.1 Presentation of data and correlations

Figure 4.9 shows the results for $\frac{h_{OGE}}{d}$ for the quintuple discharge experiment. Empirical correlations were developed for critical height of each branch during a quintuple discharge condition. They consist of following relations:

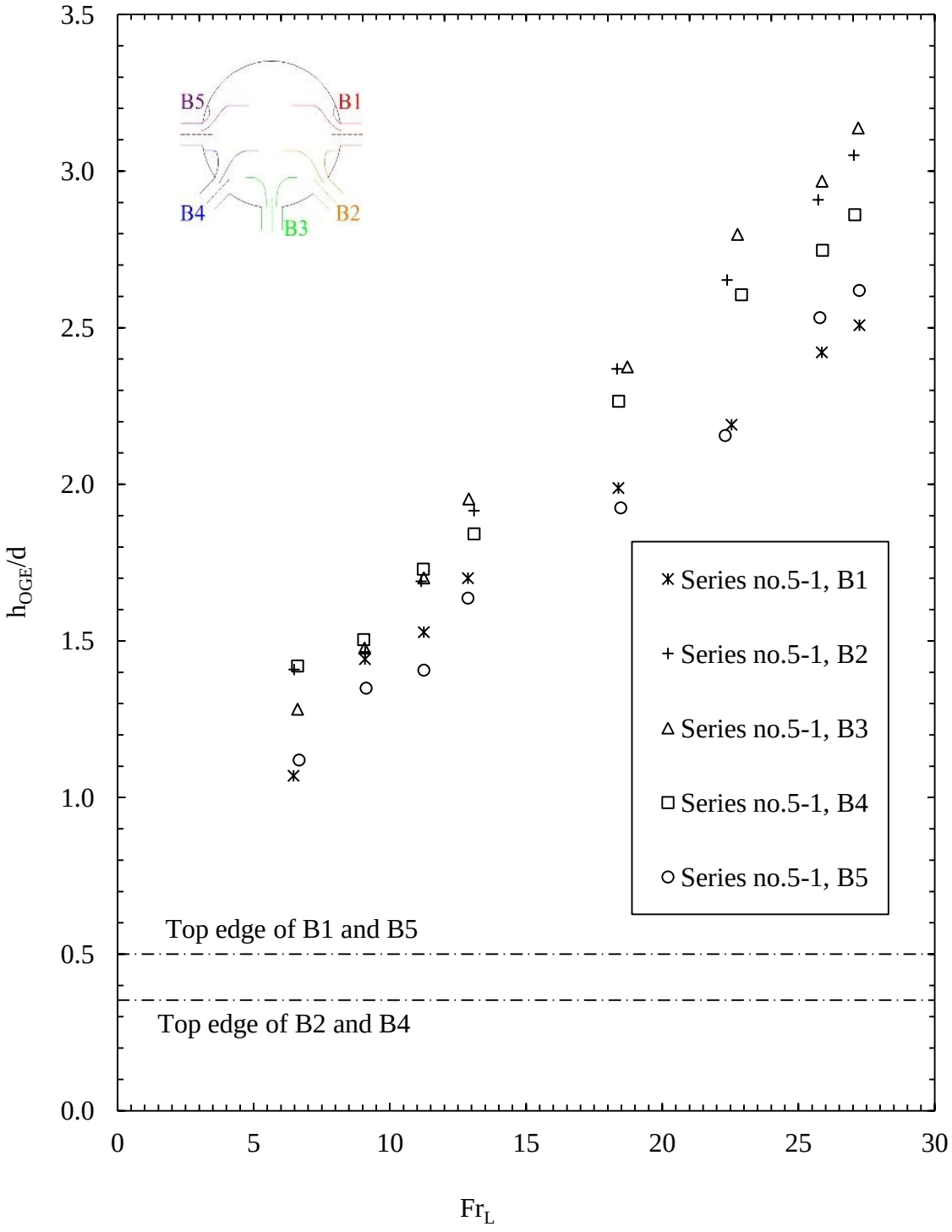

Figure 4.9: Interface level at the OGE of quintuple discharge experiment, series no. 5-1

Case no. 5: Activated two side branches, two inclined branches and a bottom branch of series no. 5-1.

For two side branches, i.e. B1 and B5 and two inclined branches, i.e. B2 and B4;

$$\frac{h_{OGE}}{d} = 0.730\ Fr_L^{0.4} \tag{4.35}$$

For bottom branch, i.e. B3;

$$\frac{h_{OGE}}{d} = 0.750\ Fr_L^{0.4} \tag{4.36}$$

For the case no. 5, the RMSD is shown in Table 4.12, when comparing the correlation and experimental values of $\frac{h_{OGE}}{d}$ over the range of branch Froude number.

It is interesting to note that C_1 of the two side branches and two inclined branches is same in series no. 5-1. The case nos. 4-C and 3-E showed that discharge from the two side branches decreased the value of C_1 to the two inclined branches and bottom branch respectively. Therefore, it was expected that C_1 of the two inclined branches and bottom branch could be lower than two side branches. However, the case no. 3-F showed that simultaneous discharge from two inclined branches and bottom branch significant increased the value of C_1 of two inclined and bottom branches. Thus, simultaneous discharges from the two inclined branches and bottom branch surpassed the effect of discharges from two side branches resulting in increased C_1 of them.

Table 4.12: Correlation constants and RMSD for quintuple discharge

Case no.	Series no.	Branch combinations					Correlation constants						RMSD (%)				
		Upper Branch/es (UB)		Middle Branch/es (MB)		Lower Branch (LB)	C_1					C_2					
		UB-1	UB-2 (opposite to UB-1)	MB-1 (below UB-1)	MB-2 (opposite to UB-1)	LB	UB-1	UB-2	MB-1	MB-2	LB		UB-1	UB-2	MB-1	MB-2	LB
5	5-1	Side -1	Side-2	Inclined-1	Inclined-2	Bottom	0.730	0.730	0.730	0.730	0.750	0.4	±7.0	±7.0	±7.0	±7.0	±14.0